RENORMALIZATION AND UNIVERSALITY OF NEURAL DYNAMICS

BO DENG

Abstract. *Spike number* is the number of spikes per burst in neural systems. A neural system is *isospiking* if the spike number is a constant integer for all bursts. Some scaling laws are derived for the corresponding code partitioning scheme. A new renormalization operator, $\mathcal{R}$, is used to demonstrate that the first natural number 1 is a universal number for the spike number code in the sense that 1 is an expanding eigenvalue of $\mathcal{R}$ and the spike number code partitioning of an appropriate stimulus parameter of any neural model is related to an approximating scheme for the eigenvalue. It is also demonstrated that $\mathcal{R}$ has a super dynamical structure having these properties: all finite dimensional dynamical systems can be conjugate embedded into the renormalization dynamics $\mathcal{R}$ on an invariant set X_0 in infinitely many ways and $\mathcal{R}$ is chaotic in X_0 which in particular has a dense orbit. It is also demonstrated that the operator $\mathcal{R}$ can contract at any rate smaller than 1 and expand at any rate greater than and equal to 1.

1. Introduction

Many neural systems can burst into spike-like activities for short periods of time. *Spike number* is the terminology given for the number of spikes per burst. It may vary with stimulatory control parameters as well as with bursts. Regarding a neural system as a communication system, it seems not unreasonable to hypothesize that the spike number can be treated as a neural discretization analog for stimulatory parameters. In fact, this particular neural code was identified in [16] as one of more than 43 other codes used by neurons, and was found as the response of a unit in the lateral line nerve of a gymnotid electric fish ([3, 15]), and more recently in the graded action potential response to glucose in pancreatic β-cells ([20]). The purpose of this paper is to provide some quantitative analysis for this *spike number code* from a dynamical system point of view.

Neural encoding and decoding is literally a dynamical process. It can be best studied by dynamical system approach as neurons can be phenomenologicaly modeled by systems of differential equations, following the seminal work of Hudgkin and Huxley ([14]). Neural encoding problem is a bifurcation problem for which changes in the stimulatory inputs or parameters cause changes in the dynamics of the systems. More specifically, consider a neural system with one stimulatory parameter changing in a predetermined direction. The spike number discretization scheme under consideration is closely related to two sequences $\{\alpha_n\}$ and $\{\omega_n\}$ defined as follows. For parameter values immediately passing α_n there are exactly n spikes

Date: August 1997–October 2000.

1991 *Mathematics Subject Classification.* 34A26, 34A47, 34C15, 34C35, 58F13, 92B20, 94A29.

Key words and phrases. Spike numbers, isospiking bifurcation, singular perturbations, natural number progression, renormalization universality, chaotic dynamics, dense orbit.

for all bursts and it is the first of such values. In contrast, ω_n is the first parameter value after α_n that the spike number differs from n for at least one burst for parameter values immediately passing ω_n. We will refer to the interval I_n bounded between α_n and ω_n *the isospiking interval of length* n. A neural system that does not have a trivial structure in I_n for its stimulus parameters may well be a system that encodes the parameters by their spike numbers.

In order for the bursting spike numbers to function as alphabets for an encoding device, many criteria must be satisfied. The scope of this paper is limited to the following two practical considerations. First, it is necessary to have a relatively small set of rules which generates $\{\alpha_n\}$ and $\{\omega_n\}$. Second, the set of non-isospiking parameter values, i.e., those for which the spike number varies with bursts, should be negligibly smaller than the isospiking ones. These criteria are certainly not necessary, but only to reflect our heuristic belief that a complex and effective communication system such as neurons may benefit greatly from having components which are the simplest and optimal to the tasks. Admittedly, there should be other criteria to consider, such as signal tuning, reliability, bandwidth efficiency. These issues, and in particular, a broader issue regarding implementation are out of the scope of this paper.

We will carry out our analysis in the context of mathematical models for neuron cells. Such models are systems of ordinary differential equations with multiple time scales, i.e., the rate of change for a subset of the equations (the fast subsystem) is significantly faster in general than that of the others (the slow subsystem). The rapid firing of spikes is associated with oscillations of the fast subsystem that vary slowly through the phase space of the slow variables. Systems of two or more time scales are singularly perturbed systems and they have been well accepted in the literature for neural system modeling, see [4], [12], [19], [22], and [17].

We will primarily consider the type of models where the burst of spikes starts at a saddle-node equilibrium point of the fast subsystem and the termination of spikes occurs at a homoclinic orbit to a saddle point. Such are models for *Tritonia* neurons, LP neurons, and pancreatic β cells, see e.g. [4], [12], [20]. The model under consideration is taken from [8] and [9]. It was constructed phenomenologically by a three-time-scale construction to mimic both qualitatively and quantitatively the experimental recordings of pancreatic β cells from [20]. The system can be regarded as a generic phenomenological model for its class. Our criterion for model selection is based more on optimal mathematical simplicity than on up-to-date physiological authenticity. We believe it is easier to use our model to extract qualitative properties of its represented class as well as quantitative properties that are model independent or universal. To the quantitative end, we will conclude by a fairly complete renormalization argument that all the scaling laws about the code partitioning sequences $\{I_n\}$ of isospiking are universal in the sense that they are either isomorphic between models or independent of any models.

Much of today's neural communication theory is build on Adrian's discoveries of *rate code* (i.e. spike frequency), *spike timing code*, and *spike frequency adaptation* phenomenon ([1]), see [18], which also contains a number of descriptions on experiments demonstrating the utilization of rate code and timing code in various neural systems. With the exception of timing code, the rate encoding and spike number encoding can be related for some cases in that the stimulus parameters are impinged differently to an otherwise same neuron model. Because of this relation, the result of this paper can be extended to these rate encoding mechanisms. We will deal with this connection somewhere else since a detailed treatment will take us too far from the main purpose of this paper.

Our approach is based on the theory of dynamical systems and bifurcations. The main strategy is to reduce the dynamics of our model system to a family of one-dimensional Poincaré return maps to which our renormalization theory can be applied. More specifically, Sec.2 is a brief mathematical derivation of the return map following the same approach as in [9]. We normalize it to a map on the unit interval $[0,1]$ with one discontinuity $c \in (0,1)$. The map is monotone increasing on the left sub-interval $[0,c)$ which corresponds to the progression of spikes. The point of discontinuity c is related to the homoclinic orbit for spike termination. The right sub-interval $[c,1]$ is associated with the quiescent phase between bursts. For parameter values from the isospiking interval I_n and for every initial point from the quiescent interval $[c,1]$, there must be exactly n subsequent iterates in the spiking interval $[0,c)$. For parameter values from a non-isospiking interval, there are initial points of $[c,1]$ that have different numbers of subsequent iterates in $[0,c)$. In other words, spike number in terms of the return map means the number of subsequent iterates in $[0,c)$ for points from $[c,1]$. This symbolic formulation for spike number gives rise to bifurcation equations for the isospiking end points α_n, ω_n in Sec.3. In Sec.4, we will focus on the family of Poincaré return maps parameterized by the singular parameter ε which usually corresponds to the slow activation rate of intracellular calcium Ca^{2+} concentration and appears in all two-time-scale models in the literature. To fix α_n and ω_n, we choose the decreasing direction of $\varepsilon \searrow 0^+$ so that $\omega_n < \alpha_n$. Main numerical findings from this section can be summarized as follows.

Sequence $\{\alpha_n\}$ and $\{\omega_n\}$ are monotone decreasing to 0^+ as $\varepsilon \searrow 0^+$ and $\alpha_{n+1} < \omega_n$. This means the ordering in the isospiking intervals $I_1 > I_2 > I_3 > \cdots$ coincides with the natural number progression ordering in their corresponding spike numbers $1, 2, 3, \ldots$. Quantitatively, these proportional scaling laws hold

$$\omega_n \sim \frac{1}{n}, \qquad |I_n| = \alpha_n - \omega_n \sim \frac{1}{n^2}, \qquad \omega_n - \alpha_{n+1} \sim \frac{1}{n} e^{-K/\omega_n},$$

where $K > 0$ is a constant, and only the proportionalities are model dependent. However the limit for the length ratio

$$\frac{|I_{n+1}|}{|I_n|} \approx 1 - \frac{2}{n} \to 1 \quad \text{as } \varepsilon \searrow 0^+,$$

is model independent.

Sec.5 is the main theoretical section, which is very much independent from other sections. Two theorems will be proved in this section. The Universal Number 1 Theorem will give conditions such that the natural number 1 as in the limit

$$1 = \lim_{n\to\infty} \frac{|I_{n+1}|}{|I_n|} = \lim_{n\to\infty} \frac{\omega_{n+1} - \omega_n}{\omega_n - \omega_{n-1}}$$

is indeed a universal constant, and so is any rational number p/q as in

$$\frac{p}{q} = \lim_{n\to\infty} \frac{\omega_{n+q} - \omega_{n+q+p}}{\omega_n - \omega_{n+q}}.$$

The arguments are based on a new renormalization operator, $\mathcal{R}$, in some functional space. We will demonstrate that the linearization of the operator at a fixed point

ψ_0 has an eigenvalue equal to 1 and that the quotient limit $(\omega_{n+1} - \omega_{n+2})/(\omega_n - \omega_{n+1}) \to 1$ is an approximation algorithm for the eigenvalue. The Superchaos Theorem also shows that (i) $\mathcal{R}$ can contract at any rate $0 < \varrho < 1$ and can expand at any rate $\varrho \geq 1$; (ii) there are infinitely many ways to conjugate any finite dimensional system to a sub-dynamics of $\mathcal{R}$ in an invariant set X_0; and (iii) the dynamical system $\{\mathcal{R}, X_0\}$ is chaotic in the sense that the set of periodic orbits is dense in X_0, it has sensitive dependence on initial conditions, and it has a dense orbit.

2. One-Dimensional Return Map

We start with the following phenomenological model for the class of neural and excitable cells for which the bursting of spikes terminates at a homoclinic orbit to a saddle point.

$$\begin{aligned}
&\dot{C} = \varepsilon(V - \varrho) \\
&\varsigma\dot{n} = (n - n_{\min})(n_{\max} - n)[(V - V_{\max}) + r_1(n - n_{\min})] - \eta_1(n - r_2) \\
&\dot{V} = (n_{\max} - n)[(V - V_{\min})(V - V_{\min} - r_3(C - C_{\min})) + \eta_2] \\
&\qquad - w(n - n_{\min}), \\
&\text{with } r_1 = \frac{V_{\max} - V_{\text{spk}}}{n_{\max} - n_{\min}},\ r_2 = \frac{n_{\max} + n_{\min}}{2},\ r_3 = \frac{V_{\text{spk}} - V_{\min}}{C_{\text{cpt}} - C_{\min}}.
\end{aligned} \tag{2.1}$$

Here, C is the slow variable for small $0 < \varepsilon \ll 1$; n and V are the fast variables of which n is faster for small $0 < \varsigma \ll 1$. $w, n_{\min}, n_{\max}, V_{\min}, V_{\text{spk}}, V_{\max}, C_{\min}, C_{\text{cpt}}, \varrho, \eta_1, \eta_2$ are parameters. In particular, $\eta_1, \eta_2, \varepsilon, \varsigma$ are non-negative small parameters which control the multiple time scale processes and $n_{\min} < n_{\max}, V_{\min} < V_{\text{spk}} < V_{\max}, C_{\min} < C_{\text{cpt}}$. We will only consider in this paper the ϱ parameter regime

$$V_{\min} < \varrho < V_{\text{spk}}$$

for which no bursts last for ever. We note that in the case of modeling the pancreatic β cells as originally motivated in [8] and [9], variable C corresponds to the intra-cellular calcium Ca^{2+} concentration, variable n measures the percentage of open potassium channels, and variable V corresponds to the cell's membrane potential. Fig.1 is a comparison between some experimental recordings on cross-membrane potentials of an islet of β-cells exposed to graded glucose concentrations and corresponding numerical simulations of the phenomenological model (2.1), mimicking the experimental data. More details on the experiment and simulation can be found in [20, 8].

Our one-dimensional map will be defined as a flow induced limiting map with $\varsigma = 0$. By the asymptotic theory of singular perturbations, the dynamics of the perturbed full system with $0 < \varsigma \ll 1$ is well approximated by that of the mapping. For this reason, only the limiting system with $\varsigma = 0$ is considered below. A detailed derivation for the map is postponed to the Appendix in order to keep our presentation more focused here. In what follows we will only describe the spiking mechanism geometrically and its relation to the map. Fig.2 is essential in guiding through the discussion.

Starting with any point near the horizontal branch of the V-shaped nullcline for the V-equation on $\mathcal{S}_1$, a typical trajectory moves in the decreasing C-direction with V barely evolving (i.e. $V(t) \approx V_{\min}$.) The time series of variable V would show

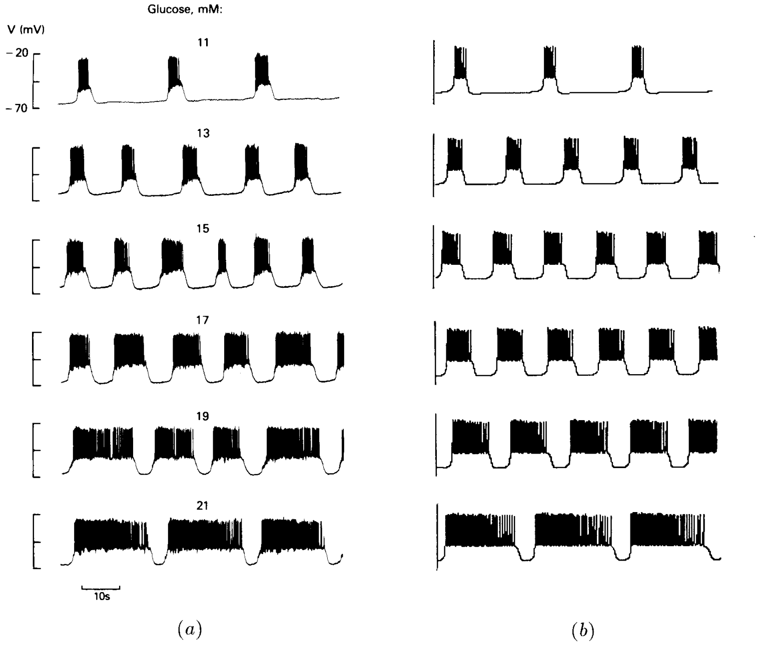

FIGURE 1. Experimental recordings (a) from [20] and numerical simulations (b) of the phenomenological model Eq.(2.1) from [8].

little change during this period of event which is referred to as *the silent* or *quiescent phase.* As soon as it clears the turning knee point K, the fast V-dynamics takes over, sending the trajectory upward quickly to the turning edge $\mathcal{T}_1$. This burst would be identified as the beginning of the first spike on the V-time series. The faster n-dynamics takes over at the $\mathcal{T}_1$ turning point, projecting the trajectory instantaneously to a point on $\mathcal{S}_2$. The trajectory then heads downward on $\mathcal{S}_2$ and connects to a point on the turning edge $\mathcal{T}_2$. The connection would be near vertical if w is near infinity, which we will assume for simplification. The last point is finally connected to a point on *the junction line* $\mathcal{J}_1 = \{V = V_{\rm spk}, n = n_{\rm min}\} \subset \mathcal{S}_1$. The net effect of the last three jumps, with the assumption that w is infinity, simply takes the trajectory's $\mathcal{T}_1$-turning point vertically down to the junction line $\mathcal{J}_1$. This would complete the first spike on the V-time series. If the junction point lies left to the orbit Γ^*, or equivalently left to *the spike termination point* $c = \Gamma^* \cap \mathcal{J}_1$, then another spike is born, giving rise to the repetitive spiking activities on the V-time series. Because $\dot{C} = \varepsilon(V - \varrho) > 0$ when $V_{\rm min} < \varrho < V_{\rm spk} \leq V$ during spiking, $C(t)$ increases with a strictly non-zero speed. Thus, the spiking trajectory will eventually land on the right side of the termination point c on $\mathcal{J}_1$ and not be able to hit the turning edge $\mathcal{T}_1$ to produce another spike before being pulled down to the horizontal branch of the V-nullcline. This would terminate the spiking activities on the V-time series and set the system to the quiescent phase again. Note that the number of spikes is exactly the number of points the trajectory hits the half interval of $\mathcal{J}_1$ left to the termination point c. Also, $c \nearrow C_{\rm cpt}$ as $\varepsilon \searrow 0^+$ and the termination

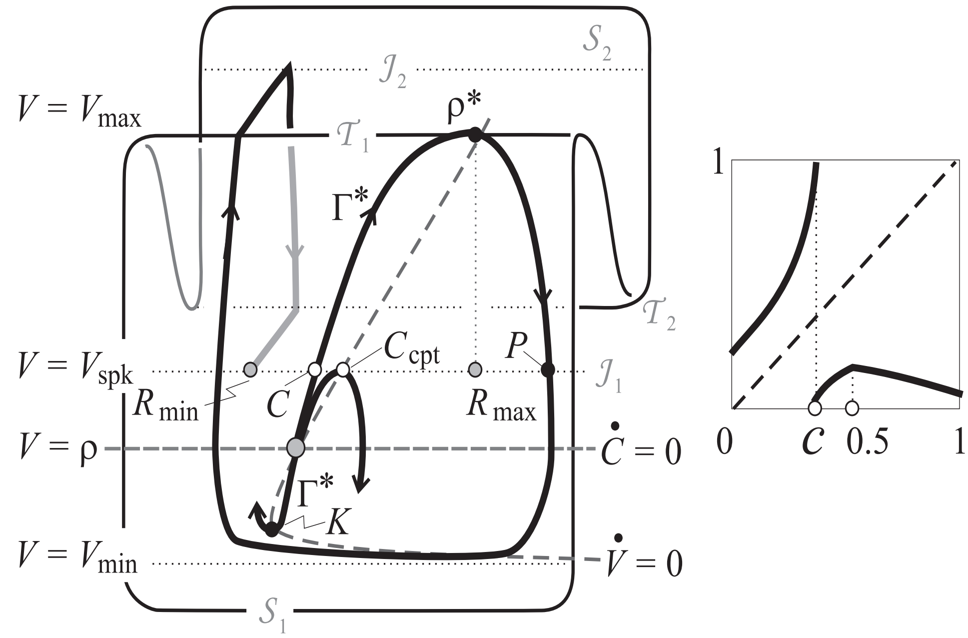

FIGURE 2. Left: Phase portrait of the limiting slow and fast subsystems. Right: A geometric graph for the return map Π.

of spikes takes place at the homoclinic orbit to C_{cpt} of the fast nV-system when $\varepsilon = 0$.

Since the reduced vector field on $\mathcal{S}_2$ are pointing downward, any line $V = \text{const.} \in (V_{\text{spk}}, V_{\max})$ on $\mathcal{S}_2$ is transversal to the flow and the Poincaré return can be defined. For the purpose of a simpler illustration, we move the cross section to the junction line $\mathcal{J}_1$ on $\mathcal{S}_1$. Although it is not transversal to the $\mathcal{S}_1$ flow, an equivalent return map is nevertheless well-defined. Specifically, a point starting on $\mathcal{J}_1$ is considered returning to $\mathcal{J}_1$ if and only if the trajectory returns by hitting $\mathcal{J}_1$ from $\mathcal{T}_2$. Thus, the *return* hit of a point originated between c and C_{cpt} is not the first two intersection points of the CV-orbit. Instead, it is the limiting point of the continued n-orbit from $\mathcal{T}_2$. Similar comment also applies to points above C_{cpt}. Note that the CV-orbit is tangent to $\mathcal{J}_1$ at C_{cpt}. We will denote by Π the return map and normalize it over the unit interval $[0, 1]$, i.e., $R_{\min} \Rightarrow 0, C_{\text{cpt}} \Rightarrow .5, R_{\max} \Rightarrow 1$. We also set $V_{\text{spk}} = 0$ from now on.

We point out a few properties which are characteristic about the map. Π is monotone increasing on $[R_{\min}, c)$ which corresponds to the spiking dynamics. It is discontinuous at the spike termination point c with the right continuous value $R_{\min}$ and the left limit $R_{\max}$. C_{cpt} is the only critical point in interval $[c, R_{\max}]$ and it is a local maximum, i.e., the map is increasing in $[c, C_{\text{cpt}}]$ and decreasing in $[C_{\text{cpt}}, R_{\max}]$. The graph is illustrated qualitatively in Fig.2.

To pursue our quantitative analysis on the spiking dynamics, we phenomenologically fit the return map Π as follows

$$\Pi(x) = \begin{cases} \varepsilon(\ell_0 - \ell_1\varrho) + x + \big[1 - (\varepsilon(\ell_0 - \ell_1\varrho) + c)\big] \times \\ \qquad \varepsilon^{b_1}|\varrho|^{b_2} \dfrac{1 - |x-c|^{1+a_1\varepsilon\varrho}}{\varepsilon^{b_1}|\varrho|^{b_2} + |x-c|}, & 0 \le x < c \\ e^{-b_3/\varepsilon}\big(1 - \Big|\dfrac{x-.5}{c-.5}\Big|^{1+a_2\varepsilon|\varrho|}\big), & c \le x < .5 \\ e^{-b_3/\varepsilon}\big(1 - \ell_2\Big|\dfrac{x}{.5} - 1\Big|^{1+a_2\varepsilon|\varrho|}\big), & .5 \le x \le 1 \end{cases} \tag{2.2}$$

where all symbols except for ϱ are positive parameters subject to these constraints:

$$V_{\min} < \varrho < V_{\text{spk}} = 0,\ 0 < \ell_2 < 1,\ b_1 > 1,\ \text{and } c = .5 + \ell_3\varepsilon\varrho.$$

A justification for the form (2.2) is given in the Appendix. Listed below are some important properties needed for the remainder sections.

The first property is that

$$\Pi(0) = \varepsilon(\ell_0 - \ell_1\varrho) + h.o.t., \tag{2.3}$$

where $h.o.t$ denotes terms of higher order than the preceding one and in the case above it is due to the constraint $b_1 > 1$. That is, $\Pi(0)$ decreases as $\varepsilon \searrow 0^+$ with a nonzero asymptotic rate $\Pi(0)/\varepsilon = (\ell_0 - \ell_1\varrho) + h.o.t. > \ell_0$. It also increases with decreasing ϱ. This follows the fact that $\dot C = \varepsilon(V-\varrho)$ for the solution through $R_{\min}$. The second property is that the graph of Π over $[0, c)$ must lie above the diagonal line $\{x_{i+1} = x_i\}$ because $\dot C = \varepsilon(V - \varrho) > 0$ for $V_{\min} < \varrho < V_{\text{spk}} \le V$ during the active phase of spiking. The third property is that

$$\lim_{\varepsilon\searrow 0^+} \Pi(x) = \begin{cases} x, & 0 \le x < .5 \\ 0, & .5 \le x \le 1. \end{cases} \tag{2.4}$$

It accounts for the fact that at the singular limit $\varepsilon = 0$, every point from $[R_{\min}, C_{\text{cpt}})$ returns to itself and the asymptotic limit of all the return points of $[C_{\text{cpt}}, R_{\max}]$ goes to $R_{\min}$. The fourth property is that the upper bound of Π over $[c, R_{\max}]$ decays exponentially as $\varepsilon \searrow 0^+$:

$$\max\{|\Pi(x)| : x \in [c, 1]\} = O(e^{-b_3/\varepsilon}). \tag{2.5}$$

This exponential scale is due to the fact that points of $[C_{\text{cpt}}, R_{\max}]$ is pulled exponentially to the quiescent branch of the V-nullcline in variable V and the time required to pass the turning point in variable C is uniformly bounded from below by an order of $1/\varepsilon$.

3. Isospiking Bifurcations

As concluded from Section 2 above, there is no persistent spiking activities for $V_{\min} < \varrho < V_{\text{spk}} = 0$. Also, if there are n spikes for a given burst, then there are precisely n iterates of Π that are in $[0, c)$, between two iterates in $[c, 1]$ which correspond to the beginning and termination of the burst. The system is said to be *isospiking* if all points of $[c, 1]$ have the same spike number, i.e., the same number of subsequent iterates in $[0, c)$.

A criterion for isospiking can be derived by following the orbits through the spike termination point c and the local maximum point C_{cpt}. To be more precise, let $x^i_{\min} = \Pi^i(c), x^i_{\max} = \Pi^i(C_{\text{cpt}})$ for $i \ge 1$. Because Π is monotone increasing in

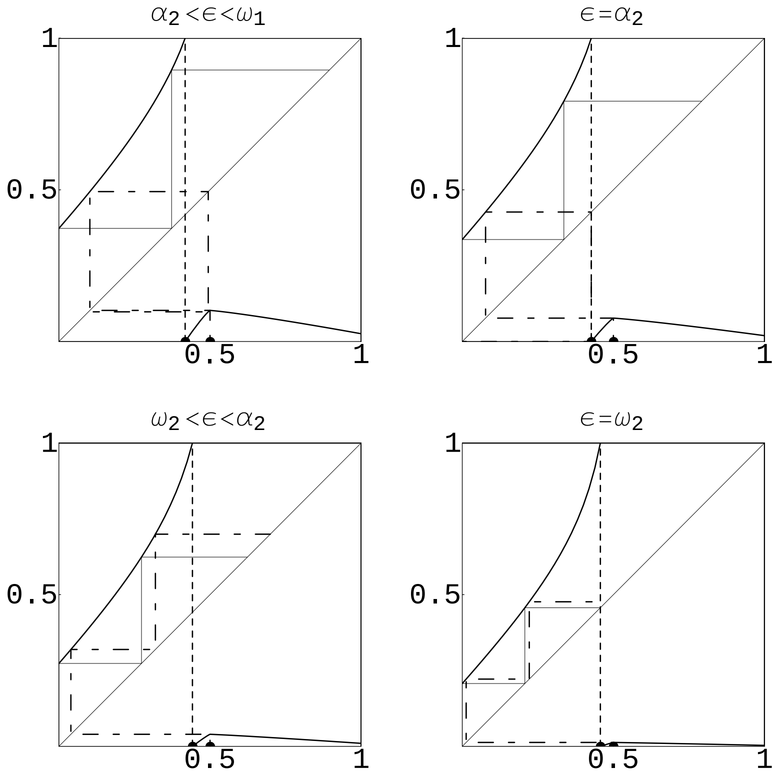

FIGURE 3. Referring clockwise from the top left phase portrait, $n = m + 1$ for the first and the third portrait and $n = m$ for the second and the fourth portrait. The systems are isospiking when $n = m$ but otherwise when $n = m + 1$. As ε descending through $\omega_1 > \alpha_2 > \omega_2$, isospiking occurs only when $\omega_2 \le \varepsilon < \alpha_2$. Spike bifurcations with other spike length are qualitative the same near the spike termination point c. All parameters except for ε are fixed for all numerical simulations. $\varrho = -0.5, \ell_0 = 0.75, \ell_1 = 0.5, \ell_2 = 0.75, \ell_3 = 0.5, a_1 = a_2 = 1, b_1 = 1.1, b_2 = 0.5, b_3 = 0.75$.

$[c, C_{\rm cpt}]$, we have $x^1_{\min} = 0 < x^1_{\max}$. We may assume from now on that $x^2_{\min} = \Pi(0) = \varepsilon(\ell_0 - \ell_1\varrho) + ... > x^1_{\max} = \Pi(C_{\rm cpt}) = O(e^{-b_3/\varepsilon})$, the maximum value of Π in $[c, 1]$. Note that the interval $[c, 1]$ is mapped onto $[0, x^1_{\max}] \subset [0, x^2_{\min}]$. Let n be the first largest integer of i so that $x^i_{\min} < c$ and m be the first largest integer of i so that $x^i_{\max} < c$. Because of the monotonicity of Π on the spiking interval $[0, c)$, we must have $x^m_{\min} < x^m_{\max}$, that is $n \ge m$. Fig.3 shows distinct spiking patterns for various combinations in $n \ge m$ and the spike termination point c. For the case $n = m$, the spike number for each point of $[c, 1]$ must be exactly n. This is because all the kth iterates for $k \le n$ are in the spiking interval $[0, c)$ for being bounded by $x^n_{\max} < c$ and the $n+1$st iterate is in the quiescent interval $[c, 1]$ for being no lesser than $x^{n+1}_{\min} \ge c$. For the other case $n > m$, we must have $n = m+1$. This is because the relation $x^1_{\max} < x^2_{\min}$ implies $x^{m+1}_{\max} < x^{m+2}_{\min}$ which in turn implies $n < m + 2$

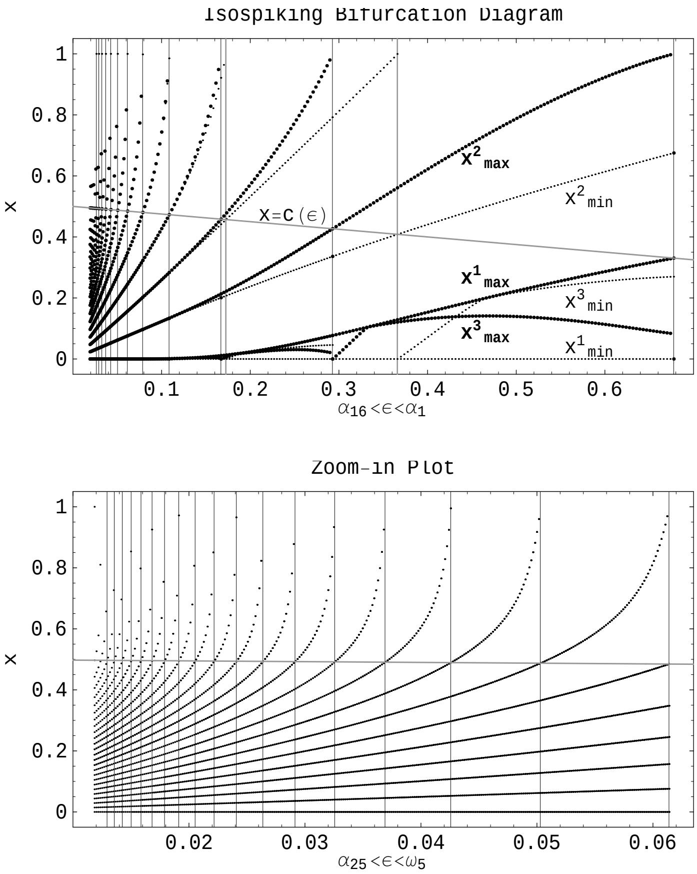

FIGURE 4. The top figure is the spike bifurcation diagram. The gray vertical lines are through ω_n below which non-isospiking sets in. The solid vertical lines are through α_n below which isospiking starts. These two types of lines are barely distinguishable from α_3 onward. The sloped gray line is the location of the spike termination point c. For parameter $\alpha_{n+1} < \varepsilon \le \alpha_n$, the first $n+1$ iterates are plotted for each of the boundary points $0 = f_\varepsilon(c)$ and $x^1_{\max} = f_\varepsilon(C_{\text{cpt}})$. The bolder dots are for $x^i_{\max}$ and the smaller dots are for $x^i_{\min}$. In $\alpha_2 < \varepsilon < \omega_1$, non-isospiking is self-evident: there are two spikes following c and one spike following C_{cpt}. Starting from α_3, these two orbits are indistinguishably close to each other, or to any other orbit. So the bottom graph only plots the last 25 of the first 50 iterates of 0.

for $x^m_{\max} < c \le x^{m+1}_{\max}$ by definition. Thus the number of iterates in $[0, c)$ differs at least for c and C_{cpt}. We can now conclude the following criterion.

Isospiking Criterion. *The system is isospiking if and only if $n = m$ which is also equivalent to*

$$x^m_{\max} < c \le x^{n+1}_{\min}.$$

We note that the system is non-isospiking if and only if $n = m+1$, i.e., $x^n_{\min} < c \le x^n_{\max}$.

From this point on, we will consider that all parameters but ε are fixed for the return map (2.2) and denote the one-parameter family by f_ε. We will choose the decreasing direction of $\varepsilon \searrow 0^+$ as preferred for bifurcation analyses. As introduced in the Introduction, the parameter values $\omega_n < \alpha_n$, if exist, mean that the system must be isospiking of length n for every $\omega_n \le \varepsilon < \alpha_n$, i.e., $x^n_{\max} < c \le x^{n+1}_{\min}$. See Fig.3. Also by definition, the parameter interval $[\omega_n, \alpha_n)$ is maximum with respect to isospiking. Because the smaller is the parameter $\varepsilon > 0$, the more spikes there are per burst. So we expect that for any given n with the property $x^n_{\max} < x^{n+1}_{\min}$, the iterates $x^n_{\max}, x^{n+1}_{\min}$ decrease with decrease in $\varepsilon \searrow 0^+$. In particular, we expect that each $x^n_{\max}$ and $x^{n+1}_{\min}$ crosses the spike termination point c in succession as $\varepsilon > 0$ decreases. Thus, the parameter value at which $x^n_{\max}$ first crosses c from above is precisely the bifurcation point $\varepsilon = \alpha_n$ where the nth isospiking begins as ε enters the interval $[\omega_n, \alpha_n)$ from above. Similarly, the parameter value at which $x^{n+1}_{\min}$ passes through c from above is the bifurcation point ω_n where the nth isospiking ends as ε leaves $[\omega_n, \alpha_n)$ from below. Hence, we can conclude that the points α_n and ω_n are determined by the following bifurcation equations:

$$f^n_{\alpha_n}(C_{\mathrm{cpt}}) = c, \quad f^{n+1}_{\omega_n}(c) = c, \quad \text{respectively.} \tag{3.1}$$

See Fig.3 and Fig.4 for illustrations.

4. Scaling Laws

The isospiking boundary points α_n and ω_n can be found numerically based on the bifurcation equations (3.1). For the one-parameter family f_ε with the other parameters fixed at the values as in Fig.3, α_n and ω_n are monotone decreasing to 0 and $\alpha_{n+1} < \omega_n$ as shown in Fig.4. To elucidate quantitative laws that determine the sequences α_n, ω_n, we further simplify the return map Π in (2.2) by dropping the term $L(x)$ in $\Pi(x) = O(\epsilon) + x + L(x)$ over the spiking interval $[0, c)$. This is motivated by the fact that for $b_1 > 2$ and outside a radius of some order ε^σ with $1 < \sigma < b_1 - 1$ from c, $L(x)$ is in the order $\varepsilon^{b_1 - \sigma}$ higher than ε. Denote such a simplification by g_ε for which $g_\varepsilon(x) = \varepsilon + x$ for $x \in [0, .5)$, $g_\varepsilon(.5) = 0$, and $\max\{g_\varepsilon(x) : x \in [.5, 1]\} = e^{-K/\varepsilon}$ for some constant $K > 0$. By using (3.1), ω_n can be calculated explicitly:

$$g^{n+1}_\varepsilon(.5) = .5 \implies g^n_\varepsilon(0) = .5 \implies n\varepsilon = .5.$$

Hence we must have $\omega_n = \frac{1}{2}\frac{1}{n}$ for the g_ε-family, i.e., in general we should expect

$$\omega_n \sim \frac{1}{n}. \tag{4.1}$$

Similarly, to calculate the $(n+1)$-isospiking starting point α_{n+1}, equation (3.1) gives

$$g^{n+1}_\varepsilon(C_{\max}) = .5 \implies g^n_\varepsilon(e^{-K/\varepsilon}) = .5 \implies n\varepsilon + e^{-K/\varepsilon} = .5,$$

where $C_{\max}$ denotes any global maximum point of g_ε in $[.5, 1]$. Thus, α_{n+1} can be approximated as

$$\alpha_{n+1} = \frac{1}{2}\frac{1}{n} - \frac{1}{n}e^{-2Kn} + h.o.t.$$

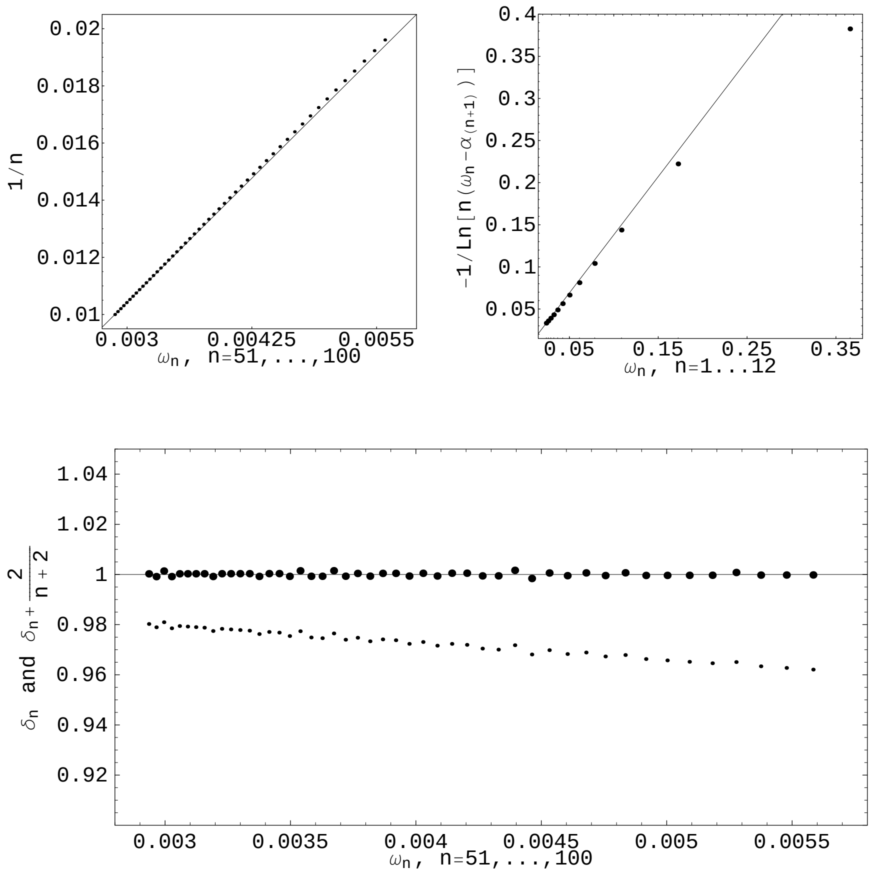

FIGURE 5. α_n and ω_n are generated for the same parameter values as in Fig.3. A program in Mathematica was written for this purpose. The strategy can be loosely described as a type of predictor-adaptation shooting method, by which one only needs to give an initial guess, minimum accuracy, and the total number of points needed. For the graph of ω_n *v.s.* $|\omega_n - \alpha_{n+1}|$, the nth non-isospiking interval length, points α_n and ω_n are accurate up to $10^{-(n+5)}$. Because the parameter K is estimated around $3/2$ for the exponentially small order of separation between α_{n+1} and ω_n, these points can be numerically separated up to $n = 16$ with the minimum margin of error. A more practically reliable guess puts the value about $n = 12$. Increasing the minimum accuracy 5 should result in separations for a larger n. The ω_n for the other two scaling graphs are accurate up to 10^{-4}.

Therefore the length of the nth non-isospiking interval is of an exponentially small order:

$$\omega_n - \alpha_{n+1} \sim \frac{1}{n} e^{-2Kn} + h.o.t.$$

Thus, in general we expect

$$\frac{-1}{\ln(n(\omega_n-\alpha_{n+1}))}\sim\frac{1}{n}\sim\omega_n. \tag{4.2}$$

These two scalings imply the following interval length ratios:

$$\frac{\omega_{n+1}-\omega_{n+2}}{\omega_n-\omega_{n+1}},\quad \frac{\alpha_{n+2}-\omega_{n+2}}{\alpha_{n+1}-\omega_{n+1}}=1-\frac{2}{n+2}+h.o.t.=1-\frac{2}{n}+h.o.t. \tag{4.3}$$

Here we note that $2/n-2/(n+2)=O(1/n^2)$.

For the ε-parameter family f_ε, these theoretical predictions are verified numerically in Fig.5 which shows the plots for ω_n *v.s.* $1/n$, ω_n *v.s.* $-1/\ln(n(\omega_n-\alpha_{n+1}))$, and ω_n *v.s.*$\delta_n=(\omega_{n+1}-\omega_{n+2})/(\omega_n-\omega_{n+1})$ in small dots and $\delta_n+2/(n+2)$ in bold dots. Only the first 12 non-isospiking intervals are sampled for the scaling law (4.2) for a numerical reason that the length for the 13th non-isospiking interval and beyond is no greater than 10^{-16} in magnitude.

We note that our return maps are not circle maps. They are not continuous either. For some diffeomorphisms on the unit circle, a bifurcation sequence similar to ω_n for the rotation numbers was studied in [2].

5. Renormalization Universality

This is the main section of the paper. The goal is to give a theoretical understanding on the universal scaling laws numerically obtained above for our neuroencode hypothesis that the per-burst spike number is coded information for neuron-to-neuron communication. Two theorems will be proved. The Universal Number 1 Theorem gives conditions for individual neural family of 1-dimensional maps that guarantee the limit

$$\frac{\omega_{n+1}-\omega_{n+2}}{\omega_n-\omega_{n+1}}\to 1 \text{ as } n\to\infty, \tag{5.1}$$

for the isospiking bifurcation sequence $\{\omega_n\}$ defined by Isospiking Criterion. In fact, it is demonstrated more generally that all positive rational numbers are universal in a similar sense. A dynamical system explanation on why this scaling law is universal leads to the introduction of a renormalization operator $\mathcal{R}$ for which 1 is a weakly expanding eigenvalue of the operator at a fixed point ψ_0 and the limit above is an approximation scheme for that eigenvalue, much in the same spirit of Feigenbaum's renormalization paradigm ([10, 11]), except that among other things ψ_0 is a nonhyperbolic fixed point and 1 is the universal number. The Superchaos Theorem shows that the stable set of ψ_0 contains an invariant set X_0 into which any finite dimensional dynamical systems can be embedded infinitely many times and X_0 has a dense orbit. It also shows that $\mathcal{R}$ can contract at any rate $0<\varrho<1$ and can expand at any rate $\varrho\ge 1$.

5.1. Universal Number 1.

We start by introducing the renormalization operator $\mathcal{R}$ and its several properties that are intended to motivate our dynamical system approach to the first theorem.

Definition 5.1. Y is the set of mappings $g:[0,1]\to[0,1]$ satisfying the following conditions (a–d):

(a) For each $g\in Y$ there is a constant $c_0^g\in(0,1]$ such that g is continuous everywhere except at $x=c_0^g$.

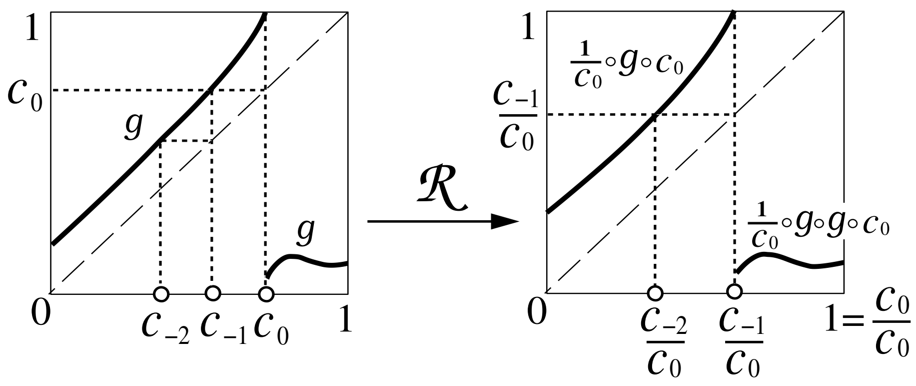

FIGURE 6. A geometric illustration for $\mathcal{R}$.

(b) g is strictly increasing in interval $[0, c_0^g)$.
(c) $g(x) \geq x$ for $x \in [0, c_0^g)$.
(d) $g(x) \leq g(0)$ for $c_0^g < x \leq 1$.

Y is equipped with the L^1 norm, hence it is a subset of the L^1 Banach space.

Remark 5.1. The value of g at the point of discontinuity c_0^g is not important because of the L^1-topology. For convenience one can set $g(c) = g(c^-) = \lim_{x\to c^-} g(x)$ with $c = c_0^g$ since the left limit always exists by the monotonicity of g in the left interval $[0, c_0^g]$. Because of this reason, any continuous increasing function g in $[0, 1]$ with $g(x) \geq x$ belongs to Y since one can consider $c_0^g = 1$. In particular, the identity function $y = id(x) = x$ is in Y. We also note that by the L^1 norm, $\|g - h\|$ simply measures the *average* distance $|g(x) - h(x)|$ over interval $[0, 1]$ between the two curves $y = g(x), y = h(x)$. If there is no confusion we will use c_0 to denote the point of discontinuity c_0^g of g.

Definition 5.2. Let

$$D = \{g \in Y : \exists c_{-1} \in (0, c_0) \text{ such that } g(c_{-1}) = c_0\}.$$

Define an operator $\mathcal{R} : D \to Y$ as follows

$$g \in D \longrightarrow \mathcal{R}[g](x) = \begin{cases} \dfrac{1}{c_0} g(c_0 x), & 0 \leq x < \dfrac{c_{-1}}{c_0} \\ \dfrac{1}{c_0} g \circ g(c_0 x), & \dfrac{c_{-1}}{c_0} \leq x \leq 1. \end{cases} \tag{5.2}$$

Remark 5.2. Though it looks like a doubling map of $\mathcal{R}[g]$ over the right interval $c_{-1}/c_0 < x \leq 1$, it is actually a composition of the left half $g_l = g|_{[0,c_0)}$ of the map with the right half $g_r = g|_{(c_0,1]}$ of the map, i.e.,

$$\frac{1}{c_0} g \circ g(c_0 x) = \frac{1}{c_0} g_r \circ g_l(c_0 x), \text{ for } \frac{c_{-1}}{c_0} \leq x \leq 1.$$

Describing it in words, one iterates g twice over the interval (c_{-1}, c_0), with the graph still below $g(0)$, and then finish the renormalization by scaling the iterated graph over $(c_{-1}, c_0]$ together with the original one over $[0, c_{-1})$ to the unit interval

$[0,1]$. See Fig.6. In terms of the Poincaré map Π as defined in (2.2), Fig.2, the renormalized $\mathcal{R}[\Pi]$ is the same as the flow induced Poincaré return map on the shorter interval $[R_{\min}, c]$, requiring only a rescaling. Two immediate properties are collected by two propositions below with the first characterizing the range and the second the iterates of $\mathcal{R}$.

Proposition 5.1. *Let $R = \{g \in Y : g(c_0) = 1\}$. Then, $\mathcal{R}[D] = R$.*

Proof. For any $g \in R$, we need to construct an $h \in D$ such that $g = \mathcal{R}[h]$. To this end, we need to define a scale down operation which is an inverse operation to $\mathcal{R}$ over a sub-interval immediately left to the point of discontinuity. More specifically, for any $0 < d < 1$ and every $g \in R$, denote

$$\mathcal{S}_d[g](x) = dg(\frac{1}{d}x),\ 0 \le x \le dc_0.$$

Now let

$$c_0^h := \frac{1}{2 - c_0}$$

and define

$$h(x) := \begin{cases} \mathcal{S}_{c_0^h}[g](x) = c_0^h g(\frac{1}{c_0^h}x), & 0 \le x < c_0 c_0^h \\ l(x) = (x - c_0 c_0^h) + c_0^h, & c_0 c_0^h \le x < c_0^h \\ c_0^h g(\frac{1-c_0}{1-c_0^h}(x - c_0^h) + c_0), & c_0^h \le x \le 1. \end{cases} \tag{5.3}$$

Figure 7 illustrates the construction of h. It is straightforward to verify that $c_{-1}^h = c_0 c_0^h$ since $h(c_{-1}^h) = l(c_{-1}^h) = c_0^h$; $\mathcal{S}_{c_0^h}[g](c_{-1}^h) = c_0^h g(c_0) = c_0^h = l(c_{-1}^h)$; $\frac{1}{c_0^h} h(c_0^h x) = g(x)$ for $x \in [0, c_0)$; $\frac{1}{c_0^h} h \circ h(c_0^h x) = g(x)$ for $x \in [c_0, 1]$, and $h(c_0^h) = 1$, both using that $c_0^h = 1/(2 - c_0)$. Hence $\mathcal{R}[h] = g$. □

Proposition 5.2.

$$\mathcal{R}^k[g](x) = \begin{cases} \frac{1}{c_{-k+1}} g(c_{-k+1}x), & 0 \le x < \frac{c_{-k}}{c_{-k+1}} \\ \frac{1}{c_{-k+1}} g^{k+1}(c_{-k+1}x), & \frac{c_{-k}}{c_{-k+1}} \le x \le 1, \end{cases}$$

where $c_{-i} = g^{-i}(c_0) \in [0, c_0)$ for all $i = 0, 1, ..., k$. More specifically, if c_0 has n backward iterates $c_{-i} = g^{-i} \in [0, c_0)$ for $i = 1, ..., n$, then the new point c_{-1}/c_0 which partitions the graph of $\mathcal{R}[g]$ into parts above the diagonal and below the point c_{-1}/c_0 has $n-1$ backward iterates $c_{-j-1}/c_0 = \mathcal{R}[g]^{-j}(c_{-1}/c_0)$ in $[0, c_{-1}/c_0)$ for $j = 1, ..., n-1$.

Proof. It follows by induction. □

A subset $U \subset D$ is *forward invariant* if $\mathcal{R}[U] \subset U$. It is *backward invariant* if there is a subset $V \subset U$ such that $\mathcal{R}[V] = U$. It is *invariant* if it is both forward and backward invariant, i.e., $\mathcal{R}[U] = U$.

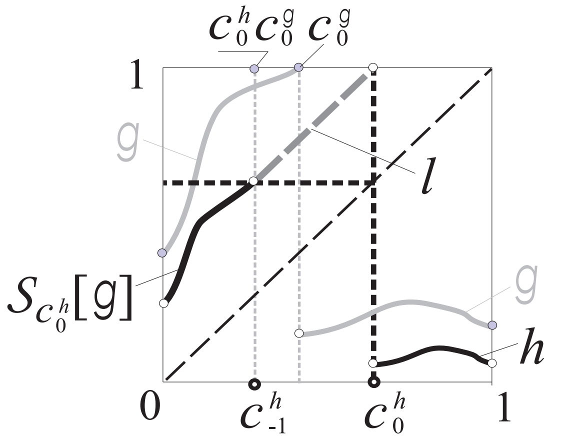

FIGURE 7. The preimage h of g is constructed by scaling g down ($\mathcal{S}_{c_0^h}[g]$), attaching a line segment l of slope 1, and scaling the right half of g accordingly over the right interval of h.

Proposition 5.3. *Let*

$$X = \{g \in Y : \exists x_* \in [0, c_0] \text{ such that } g(x_*^-) = x_*\}$$
$$\Sigma_n = \{g \in R \subset Y : g^{-k}(c_0) = c_{-k} \in [0, c_0) \text{ for } 1 \le k \le n \text{ such that } 0 = c_{-n} < c_{-n+1} < \cdots < c_0\},$$

where $g(x_*^-) = \lim_{x \to x_*^-} g(x)\}$. *Then*

(a) $X \subset D$ *is forward invariant and* $\mathcal{R}[X]$ *is invariant, i.e.,* $\mathcal{R}^2[X] = \mathcal{R}[X]$.
(b) X *contains all forward invariant subsets of* Y *under* $\mathcal{R}$.
(c) $\Sigma_{n+1} = \mathcal{R}^{-n}[\Sigma_1]$ *and more generally,* $\mathcal{R}^k[\Sigma_{n+k}] = \Sigma_n$.

Proof. For $g \in X$, let $x_g = \sup\{x_* \in [0, c_0] : x_* = g(x_*^-)\}$. Then we also have $x_g = g(x_g^-)$. So without loss of generality, assume $x_* = x_g$ is the largest fixed point of g in $[0, c_0]$ for statement (a). If $x_* < c_0$, then $g(x) > x$ for $x_* < x \le c_0$. So $c_k = g^{-k}(c_0)$ exist for all $k \ge 1$ and $c_0 > c_{-1} > \cdots \to x_*$. Thus $g \in D$ and $\mathcal{R}[g] \in X$ with the scaled fixed point x_*/c_0. If $x_* = c_0$, then $\mathcal{R}[g]$ has 1 as its fixed point. In either cases we have $\mathcal{R}[g] \in X$ and X is forward invariant. Hence, $\mathcal{R}^2[X] \subset \mathcal{R}[X] \subset X$. To show $\mathcal{R}[X]$ is backward invariant, take any $g \in \mathcal{R}[X] \subset R = \mathcal{R}[D]$. By Proposition 5.1 there is an $h \in D$ such that $\mathcal{R}[h] = g$. By the construction of h from (5.3), we see that h has a scaled-down fixed point $x_* c_0^h$. Thus, $h \in X$. Since $h(c_0^h) = 1$ from the construction in Proposition 5.1, we have $h \in R$ and $h \in \mathcal{R}[X]$. Hence, (a) holds.

If $g \in U$ and U is forward invariant, then $\mathcal{R}^k[g]$ exists for all $k \ge 0$. That is, $g^{-k}(c_0) = c_{-k}$ exist for all $k \ge 1$ with $0 \le \cdots < c_{-k} \le c_{-k+1} \le \cdots \le c_0$. Thus $\lim_{k\to\infty} c_k = x_* \in [0, c_0]$ exists and $g(x_*) = x_*$. So $g \in X$ and $U \subset X$ holds. This shows (b).

If $g \in \Sigma_{n+1}$, then $0 = c_{-n-1} \le c_{-n} \le \cdots \le c_{-1} \le c_0$. By Proposition 5.2, $\mathcal{R}^n[g]$ exists with the discontinuity at c_{-n}/c_{-n+1} and the discontinuity's perimage at $c_{-n-1}/c_{-n+1} = 0$. This shows $\mathcal{R}^n[g] \in \Sigma_1$ by definition. Thus, $\Sigma_{n+1} \subset \mathcal{R}^{-n}[\Sigma_1]$.

To show $\Sigma_{n+1} \supset \mathcal{R}^{-n}[\Sigma_1]$, we need to show that for any $g \in \Sigma_1$, there is an $\bar{h} \in \Sigma_{n+1}$ such that $\mathcal{R}^n[\bar{h}] = g$. Since $g \in \Sigma_1 \subset R$, we can construct an h by (5.3) of Proposition 5.1 for which $\mathcal{R}[h] = g$. From the construction of h we can conclude that $c_0^h = 1/(2-c_0^g), c_{-1}^h = c_0^g c_0^h$, and $c_{-2}^h = c_{-1}^g c_0^h = 0$ since $g \in \Sigma_1$. Also, $h(c_0^h) = 1$. So $h \in \Sigma_2$. Applying the same inverse procedure to h recursively we can find $\bar{h} \in \Sigma_{n+1}$ such that $\mathcal{R}^n[\bar{h}] = g$. So $\Sigma_{n+1} \supset \mathcal{R}^{-n}[\Sigma_1]$. The general identity of (c) can be verified similarly. This completes (c). □

The following result simply says that $\{\Sigma_n\}$ converges to X point-wise uniformly over $[0,1]$.

Proposition 5.4. *For each $g \in X$, there is a sequence $g_n \in \Sigma_n$ such that $g_n \to g$ uniformly in $[0,1]$.*

Proof. Let $g \in X$. Define

$$g_\mu(x) := \begin{cases} g(x), & \text{when } g(x) \geq x+\mu \text{ and } x \in [0, c_0) \\ x+\mu, & \text{when } g(x) \leq x+\mu \text{ and } x \in [0, c_0) \\ g(x), & x \in (c_0, 1]. \end{cases}$$

It is straightforward to verify that $g_\mu(x) \in x$ for small $\mu > 0$ for $x \in [0, c_0)$. By intermediate value theorem there exists a decreasing sequence $\{\mu_n\}$ for sufficiently large n such that $\mu_n \to 0$ and $g_{\mu_n}^n(0) = c_0$, i.e., $g_{\mu_n} \in \Sigma_n$. The convergence that $g_{\mu_n} \to g$ is obviously uniformly over the interval $[0,1]$. □

Proposition 5.5. *Let*

$$W_{id}^u := \{\psi_\mu : 0 \leq \mu \leq 1/2\} \text{ with } \psi_\mu(x) = \begin{cases} \mu + x, & 0 \leq x < 1-\mu \\ 0, & 1-\mu \leq x \leq 1. \end{cases}$$

Then

(a) *$id = \psi_0$ is a fixed point of $\mathcal{R}$.*
(b) *W_{id}^u is backward invariant with $\mathcal{R}[\psi_\mu] = \psi_{\mu/(1-\mu)}$.*
(c) *$\mathcal{R}$ is weakly expanding along W_{id}^u in the sense that*

$$\|\mathcal{R}[\psi_\mu] - \psi_0\| > \|\psi_\mu - \psi_0\|.$$

(d) *1 is an eigenvalue of $\mathcal{R}$'s linearization at ψ_0 and the unit eigenvector is given as*

$$u_0(x) := \frac{1}{2}s_1(x) - \frac{1}{2}\delta_1(x),$$

where $s_1(x) = 1, 0 \leq x < 1$ and $s_1(1) = 0$, i.e. $s_1 \equiv 1$ in L^1, and δ_1 is the delta distribution function, i.e., $\delta_1(x) = 0, x \neq 1$, $\delta_1(1) = \infty$, and $\int_{1-a}^{1+a} \phi(x)\delta_1(x)dx = \phi(1)$ for any C^0 test function ϕ, and any $0 < a \leq \infty$.

Proof. It is straightforward to verify (a) as well as (b):

$$\mathcal{R}[\psi_\mu] = \psi_{\mu/(1-\mu)}, \text{ and equivalently, } \mathcal{R}^{-1}[\psi_\mu] = \psi_{\mu/(1+\mu)}.$$

It is not forward invariant because it requires $\mu/(1-\mu) < 1/2$, or $\mu < 1/3$. That is, with $V = \{\psi_\mu : 0 \leq \mu < 1/3\} \subset W_{id}^u$ we have $\mathcal{R}[V] = W_{id}^u$.

To show (c), a more general relation holds as follows

$$\|\psi_\mu - \psi_0\| > \|\psi_\zeta - \psi_0\| \text{ if } \mu > \zeta \geq 0.$$

In fact, since in general $\|\psi_\mu - \psi_\lambda\|$ is the area between the two curves that consists of the area of a parallelogram and the area of a trapezoid, we have thus by elementary calculations

$$\|\psi_\mu - \psi_\lambda\| = (\mu-\lambda)\big(\frac{4+\lambda-3\mu}{2}\big) \sim (\mu-\lambda), \text{ assuming } \mu > \lambda \geq 0. \tag{5.4}$$

In particular, with $\lambda = 0$, we have

$$\|\psi_\mu - \psi_0\| = \mu\frac{4-3\mu}{2},$$

which is increasing in $\mu \in [0, 2/3] \supset [0, 1/2]$. Since $\mathcal{R}[\psi_\mu] = \psi_{\mu/(1-\mu)}$ by (b), (c) is verified.

Again by (b) and expression (5.4), we have

$$\begin{aligned}\|\mathcal{R}[\psi_\mu] - \mathcal{R}[\psi_0] - 1\cdot(\psi_\mu - \psi_0)\| &= \|\psi_{\mu/(1-\mu)} - \psi_\mu\| \\ &= \Big(\frac{\mu}{1-\mu} - \mu\Big)\frac{4-3\mu}{2} \\ &\sim \mu^2 \sim \|\psi_\mu - \psi_0\|^2,\end{aligned}$$

showing the derivative of $\mathcal{R}$ at ψ_0 in the direction of W^u_{id} is the unitary operator in L^1, and 1 is the eigenvalue. As for the unit eigenvector u_0 we have

$$\begin{aligned} u_\mu := \frac{\psi_\mu - \psi_0}{\|\psi_\mu - \psi_0\|} &= \begin{cases} \dfrac{2}{4-3\mu}, & 0 \leq x < 1-\mu \\ \dfrac{-2x}{\mu(4-3\mu)}, & 1-\mu < x \leq 1 \end{cases} \\ &= \begin{cases} \dfrac{2}{4-3\mu}, & 0 \leq x < 1-\mu \\ 0, & 1-\mu < x \leq 1 \end{cases} + \begin{cases} 0, & 0 \leq x < 1-\mu \\ \dfrac{-2x}{\mu(4-3\mu)}, & 1-\mu < x \leq 1 \end{cases} \\ &\to \frac{1}{2}s_1(x) - \frac{1}{2}\delta_1(x) = u_0(x), \text{ as } \mu \to 0. \end{aligned}$$

This proves (d). ☐

Proposition 5.6. (a) *$\gamma = \{\psi_{1/n}\}, n \geq 2$, is a backward orbit of $\mathcal{R}$ starting at $\psi_{1/2}$.*

(b) *$\psi^n_\mu(0) = c_0 = 1-\mu$ if and only if $\mu = 1/(n+1)$, i.e., $\psi_{1/(n+1)} \in \Sigma_n$.*

(c) *$\omega_n = \alpha_{n+1} = 1/(n+1)$, that is, ψ_μ is isospiking of length n if and only if $1/(n+1) \leq \mu < 1/n$.*

(d)
$$\frac{\omega_{n+1} - \omega_{n+2}}{\omega_n - \omega_{n+1}} = 1 - \frac{2}{n} + h.o.t \to 1 \text{ as } n \to \infty.$$

(e)
$$\begin{aligned} \|\psi_{1/n} - \psi_0\| &= \frac{1}{n}(2 - \frac{3}{2n}), \text{ and} \\ \frac{\|\psi_{1/(n+2)} - \psi_{1/(n+1)}\|}{\|\psi_{1/(n+1)} - \psi_{1/n}\|} &= 1 - \frac{2}{n+2} + h.o.t \\ &= 1 - \frac{2}{n} + h.o.t \to 1 \text{ as } n \to \infty. \end{aligned}$$

Proof. Statement (a) holds because by the proof of Proposition 5.5 we have $\mathcal{R}[\psi_\mu] = \psi_{\mu/(1-\mu)}$ and the identity

$$\frac{\frac{1}{n}}{1+\frac{1}{n}} = \frac{1}{n+1}.$$

Statement (b) holds because $\psi_\mu^n(0) = n\mu = c_0 = 1-\mu$ iff $\mu = 1/(n+1)$. Statement (c) follows from the Isospiking Criterion of Sec.3. Statement (d) is straightforward. Finally, (e) follows from the expression (5.4). □

Notice that by the expression (5.4), $\|\psi_{1/(n+1)} - \psi_{1/n}\| \sim (1/n - 1/(n+1)) = \omega_{n-1} - \omega_n$. Thus (d) and (e) are essentially the same. Also statement (e) re-confirms the fact that 1 is the eigenvalue along the direction W^u_{id} and taking the limit of the quotient difference

$$\frac{\omega_{n+1} - \omega_{n+2}}{\omega_n - \omega_{n+1}} \to 1$$

is an approximation scheme for the eigenvalue.

Universal Number 1 Theorem. *Let $\{f_\mu\}$ with $0 \le \mu \le m_0 \ll 1$ be a one-parameter family in Y, where m_0 is a sufficiently small constant and $f_\mu \in Y$ for all $\mu \in [0, m_0]$. Let $c_0^\mu = c_0^{f_\mu} \in (0,1]$ with $\mu \in [0, m_0]$ denote the discontinuity of f_μ and $c_{-k}^\mu = f_\mu^{-k}(c_0^\mu)$ be the kth back iterate of c_0^μ. Assume the following conditions are satisfied*

(a) *There exist an integer $k_0 \ge 1$ and a constant c_1 such that*

$$c^\mu_{-k_0+1} = c_0^0 + c_1\mu + o(\mu)$$

for $\mu \in [0, m_0]$.

(b) *There exist some constants $a_1 > 0, a_2$ such that*

$$f_\mu(x) = x + a_1\mu + a_2\mu^2 + o(\mu^2) \text{ for } x \in [0, c^\mu_{-k_0}] \text{ and } \mu \in [0, m_0].$$

Then there exists a unique monotone decreasing sequence $\{\omega_n\}$ with $\omega_n \to 0$ such that

$$f_{\omega_n} \in \Sigma_n \text{ and } \frac{\omega_{n+1} - \omega_{n+2}}{\omega_n - \omega_{n+1}} \to 1 \text{ as } n \to \infty. \tag{5.5}$$

More generally, for any pair of integers $p \ge 0$ and $q > 0$ we have

$$\frac{\omega_{n+q} - \omega_{n+q+p}}{\omega_n - \omega_{n+q}} \to \frac{p}{q} \text{ as } n \to \infty. \tag{5.6}$$

Remark 5.3. By the assumptions (a,b) above, neural families are distinguished by the parameters c_0^μ, c_1, a_1, a_2, and the higher order terms in their expansion at $\mu = 0$. They all share the same property that $f_\mu(x) \to x$ as $\mu \to 0$, which is the main cause for the stated universality.

Proof. The proof will be done by mainly considering the k_0th renormalized family $g_\mu = \mathcal{R}^{k_0}[f_\mu]$. Consider $g_\mu(x)$ in the left half interval $x \in [0, \bar{c}_0^\mu]$ only, we have by Proposition 5.2 and both hypotheses (a, b),

$$\begin{aligned} g_\mu(x) &= x + \frac{1}{c^\mu_{-k_0+1}}(a_1\mu + a_2\mu^2 + o(\mu^2)) \\ &= x + \bar{a}_1\mu + \bar{a}_2\mu^2 + o(\mu^2) \end{aligned}$$

where $\bar{a}_1 = a_1/c_0^0 > 0$ and $\bar{a}_2$ is a constant depending on a_1, a_2, c_0^0, c_1, obtained by collecting the coefficients of μ-term and μ^2-term respectively in g_μ. Denote the discontinuity of g_μ by

$$\bar{c}_0^\mu = \frac{c_{-k_0}^\mu}{c_{-k_0+1}^\mu}.$$

Then from the expression of g_μ and the equation $g_\mu(\bar{c}_0^\mu) = 1$ we obtain

$$\bar{c}_0^\mu = 1 - (\bar{a}_1\mu + \bar{a}_2\mu^2 + o(\mu^2)) := 1 + b_1\mu + o(\mu),$$

where $b_1 = -\bar{a}_1$.

By definition, $g_\mu \in \Sigma_n$ if and only if $g_\mu^n(0) = \bar{c}_0^\mu = 1 + b_1\mu + o(\mu)$. It is by induction to get

$$g_\mu^n(0) = n(\bar{a}_1\mu + \bar{a}_2\mu^2 + o(\mu^2)).$$

Thus solving $g_\mu^n(0) = \bar{c}_0^\mu$ is equivalent to solving

$$\begin{aligned}\theta(\mu) :&= g_\mu^n(0) - \bar{c}_0^\mu \\ &= n(\bar{a}_1\mu + \bar{a}_2\mu^2 + o(\mu^2)) - (1 + b_1\mu + o(\mu)) = 0\end{aligned}$$

This is done by showing that for each sufficiently large n, θ is increasing in μ with the property that $\theta(0) = -1 < 0$ and $\theta(m_0) > 0$. Therefore there is a unique solution denoted by

$$\mu = \bar{\omega}_n.$$

To approximate $\bar{\omega}_n$, we assume it takes the following form

$$\bar{\omega}_n = \frac{r_1}{n} + \frac{r_2}{n^2} + o(\frac{1}{n^2}).$$

Substituting this form into the equation $g_\mu^n(0) = \bar{c}_0^\mu$, approximating the equation to order $o(\frac{1}{n})$ by equating the constant and $1/n$ terms on both sides, we find

$$r_1 = \frac{1}{\bar{a}_1} \text{ and } r_2 = \frac{b_1 r_1 - \bar{a}_2 r_1^2}{\bar{a}_1}.$$

Now for any integer pair $p \geq 0$ and $q > 0$ we have by elementary simplification

$$\begin{aligned}\frac{\bar{\omega}_{n+q} - \bar{\omega}_{n+q+p}}{\bar{\omega}_n - \bar{\omega}_{n+q}} &= \frac{\frac{r_1}{n+q} + \frac{r_2}{(n+q)^2} + o(\frac{1}{n^2}) - \Big(\frac{r_1}{n+q+p} + \frac{r_2}{(n+q+p)^2} + o(\frac{1}{n^2})\Big)}{\frac{r_1}{n} + \frac{r_2}{n^2} + o(\frac{1}{n^2}) - \Big(\frac{r_1}{n+q} + \frac{r_2}{(n+q)^2} + o(\frac{1}{n^2})\Big)} \\ &= \frac{n(n+q)}{(n+q)(n+q+p)} \frac{pr_1 + r_2\frac{p(2n+2q+p)}{(n+q)(n+p+q)} + o(1)}{qr_1 + r_2\frac{q(2n+q)}{n(n+q)} + o(1)} \\ &\to \frac{p}{q} \text{ as } n \to \infty.\end{aligned}$$

Finally, we notice that due to renormalization, $g_\mu = \mathcal{R}^{k_0}[f_\mu] \in \Sigma_n$ if and only if $f_\mu \in \Sigma_{n+k_0}$ by Proposition 5.3. Therefore we can conclude that $\omega_{n+k_0} = \bar{\omega}_n$ and the limit

$$\frac{\omega_{n+q} - \omega_{n+q+p}}{\omega_n - \omega_{n+q}} \to \frac{p}{q} \text{ as } n \to \infty$$

holds as desired. This proves the theorem. □

Proposition 5.7. *The universality (5.5) implies the universality (5.6).*

Proof. In fact, the limit (5.5) implies the following two limits: For any fixed integers $m \geq 0, k > 0$, we have

$$\frac{\omega_{n+m} - \omega_{n+m+1}}{\omega_n - \omega_{n+1}} = \prod_{i=1}^{m} \frac{\omega_{n+i} - \omega_{n+i+1}}{\omega_n + (i-1) - \omega_{n+i}} \to \prod_{i=1}^{m} 1 \text{ as } n \to \infty,$$

and

$$\frac{\omega_{n+m} - \omega_{n+m+k}}{\omega_n - \omega_{n+1}} = \sum_{j=0}^{k-1} \frac{\omega_{n+m+j} - \omega_{n+m+j+1}}{\omega_n - \omega_{n+1}} \to \sum_{j=0}^{k-1} 1 = k \text{ as } n \to \infty.$$

Hence, we have the universality limit (5.6):

$$\frac{\omega_{n+q} - \omega_{n+q+p}}{\omega_n - \omega_{n+q}} = \frac{(\omega_{n+q} - \omega_{n+q+p})/(\omega_n - \omega_{n+1})}{(\omega_n - \omega_{n+q})/(\omega_n - \omega_{n+1})} \to \frac{p}{q} \text{ as } n \to \infty.$$

□

We note that X contains $id = \psi_0$ and is forward invariant. It is large enough to contain infinitely many co-dimension-one subspaces of Y. For example, let $E_{x_0} : Y \to \mathbb{R}$ be the functional such that $E_{x_0}(g) = g(x_0) - x_0$. Then the subspace $\{g \in Y : E_{x_0}(g) = 0\}$ is at least of co-dimension-one in X. On the other hand, W^u_{id} is a 1-dimensional manifold that is not in X. So X is a subset of Y that is not smaller than co-dimension-one space but smaller than the full space. In any case, X is the center-stable set and W^u_{id} is the (weak) unstable manifold of the non-hyperbolic fixed point $id = \psi_0$. Thus, similar to λ-lemmas of non-hyperbolic fixed points from [7], we should expect the following: For any continuous one-parameter family $\{f_\mu\} \subset Y$ of mappings that intersects the stable set X transversely at f_0, if $\mathcal{R}^n[f_0] \to id = \psi_0$, then $\mathcal{R}^n[\{f_\mu\}]$ must converge to the unstable manifold W^u_{id} as $n \to \infty$. The following result is a weaker form of such λ-lemmas.

Inclination Lemma. *Let $\{f_\mu\}$ with $0 \leq \mu \leq m_0 \ll 1$ be a one-parameter family in Y, where m_0 is a sufficiently small constant and $f_\mu \in Y$ for all $\mu \in [0, m_0]$. Let $c_0^\mu = c_0^{f_\mu} \in (0, 1]$ with $\mu \in [0, m_0]$ denote the discontinuity of f_μ and $c_{-k}^\mu = f_\mu^{-k}(c_0^\mu)$ be the kth back iterate of c_0^μ. Assume the following conditions are satisfied*

(a) *There exist an integer $k_0 \geq 1$ and a constant c_1 such that*

$$c_{-k_0+1}^\mu = c_0^0 + c_1\mu + o(\mu)$$

for $\mu \in [0, m_0]$.

(b) *There exists a constant $a_1 > 0$ such that*

$$f_\mu(x) = x + a_1\mu + o(\mu) \text{ for } x \in [0, c_{-k_0}^\mu] \text{ and } \mu \in [0, m_0].$$

(c)

$$f_\mu(x) = O(\mu) \text{ for } x \in (c_0^\mu, 1] \text{ and } \mu \in [0, m_0].$$

Then for any μ_0, and any $\epsilon > 0$, there is an integer N_0 such that for any iterate $n > N_0$, there is a $\mu \in (0, m_0]$ sufficiently small satisfying the following

$$\|\mathcal{R}^n[f_\mu] - \psi_{\mu_0}\| < \epsilon,$$

where ψ_μ defines the backward invariant, expanding family through id constructed in Proposition 5.5.

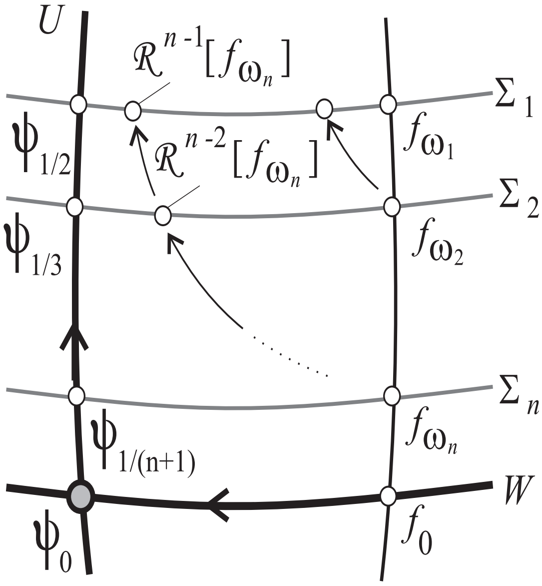

FIGURE 8. A geometric view of the dynamics near the fixed point ψ_0. Notice that the closer f_{ω_n} is to $W = X$, the closer $\mathcal{R}^{n-1}[f_{\omega_n}]$ is to the point $\psi_{1/2}$ on $U = W^u_{id}$. See also Fig.9.

Proof. Figure 8 gives a graphical illustration for the lemma. Similar to the proof of the Universal Number 1 Theorem, the proof is carried out by mainly considering the k_0th renormalized family $g_\mu = \mathcal{R}^{k_0}[f_\mu]$. Denote the discontinuity of g_μ by $\bar{c}_0^\mu$. By Proposition 5.2 and hypotheses (a, c), we have

$$g_\mu(x) = O(\mu) \text{ for } x \in (\bar{c}_0^\mu, 1] \text{ and } \mu \in [0, m_0],$$

because the outer most composition in $f_\mu^{k_0+1}(c^\mu_{-k_0+1}x)/c^\mu_{-k_0+1}$ is of order $O(\mu)$ and $c^\mu_{-k_0+1} = O(1)$. Consider $g_\mu(x)$ in the left half interval $x \in [0, \bar{c}_0^\mu]$ next, we have by Proposition 5.2 and both hypotheses (a, b),

$$\begin{aligned} g_\mu(x) &= x + \frac{1}{c^\mu_{-k_0+1}}(a_1\mu + o(\mu)) \\ &= x + \bar{a}_1\mu + o(\mu) \end{aligned}$$

where $\bar{a}_1 = a_1/c_0^0 > 0$ is a constant similar to the proof of the preceding theorem. Denote

$$\bar{c}^\mu_{-k} = g_\mu^{-k}(\bar{c}_0^\mu),$$

whenever defined. For simpler notation we denote

$$c_{-k} = \bar{c}^\mu_{-k} \text{ for } k = 0, 1, 2, \dots,$$

and

$$a = \bar{a}_1.$$

Since $g_\mu \in \mathcal{R}[D] = R$, $g_\mu(c_0) = 1$ (using the simplified notation $c_0 = \bar{c}_0^\mu$), and thus

$$g_\mu^{k+1}(c_{-k}) = c_{-k} + (k+1)(a\mu + o(\mu)) = 1.$$

Thus

$$c_{-k} = 1 - (k+1)(a\mu + o(\mu)) \text{ and } c_0 = 1 - (a\mu + o(\mu)).$$

By Proposition 5.2,

$$\mathcal{R}^k[g_\mu](x) = x + \frac{a\mu + o(\mu)}{c_{-k+1}} \text{ for } 0 \le x \le \frac{c_{-k}}{c_{-k+1}}.$$

The rest of the proof is to show that a μ satisfying the following equation

$$\frac{a\mu}{c_{-k+1}} = \mu_0 \tag{5.7}$$

is what we look for. By using the expression for c_{-k}, the equation above is solved to give

$$\mu = \frac{\mu_0}{a + k\mu_0(a + o(1))} = O(\frac{1}{k}) \to 0 \text{ as } k \to \infty.$$

We are now ready to estimate $\|\mathcal{R}^k[g] - \psi_{\mu_0}\|$. The difference is the area between the two curves $h = \mathcal{R}^k[g_\mu]$ and ψ_{μ_0} which can be divided into three regions for consideration: (i) The parallelogram between $h = \mathcal{R}^k[g_\mu]$ and ψ_{μ_0} over the interval $[0, \min\{c_0^h, 1-\mu_0\}]$; (ii) the trapezoid-like region between the two curves over the interval $[\min\{c_0^h, 1-\mu_0\}, \max\{c_0^h, 1-\mu_0\}]$; (iii) the region between h and the x-axis over the interval $[\max\{c_0^h, 1-\mu_0\}, 1]$ for which the height of the curve h is of order $O(\mu)$. Our task is to show that each of the three areas is of order $o(1)$ as $\mu = O(1/k) \to 0$. First there is no additional argument needed for the region (iii) because $h = O(\mu)$ over the corresponding sub-interval of $[0,1]$. For region (i), because of the choice of μ from the equation $a\mu/c_{-k+1} = \mu_0$, we have that the difference between the two curves h and ψ_{μ_0} over that interval is

$$\begin{aligned}
|h(x) - \psi_{\mu_0}| &= |\frac{a\mu + o(\mu)}{c_{-k+1}} - \mu_0| = \frac{o(\mu)}{c_{-k+1}} \\
&= \frac{a\mu}{c_{-k+1}} \frac{o(\mu)}{a\mu} = \mu_0 o(1) \text{ (because } \frac{a\mu}{c_{-k+1}} = \mu_0 \text{ by Eq.(5.7))} \\
&= o(1) \text{ as } \mu \to 0.
\end{aligned}$$

For region (ii), the function difference between h and ψ_{μ_0} is of order $O(1)$. However, the length of the interval $[\min\{c_0^h, 1-\mu_0\}, \max\{c_0^h, 1-\mu_0\}]$ is small. In fact, the length of the interval is

$$\begin{aligned}
|c_0^h - 1 + \mu_0| &= |\frac{c_{-k}}{c_{-k+1}} - 1 + \mu_0| = |\frac{c_{-k} - c_{-k+1} + \mu_0 c_{-k+1}}{c_{-k+1}}| \\
&= |\frac{c_{-k} - c_{-k+1} + a\mu}{c_{-k+1}}| \text{ (because } \mu_0 c_{-k+1} = a\mu \text{ by Eq.(5.7))} \\
&= |\frac{-a\mu - o(\mu) - a\mu}{c_{-k+1}}| \text{ (because } c_{-k+1} = g_\mu(c_{-k}) = c_{-k} + a\mu + o(\mu)) \\
&= |\frac{o(\mu)}{c_{-k+1}}| = o(1),
\end{aligned}$$

where the last estimate follows from the same argument as above for region (i). Combining the three estimates together, we can conclude that

$$\|\mathcal{R}^k[g_\mu] - \psi_{\mu_0}\| = o(1) \text{ as } \mu = O(\frac{1}{k}) \to 0.$$

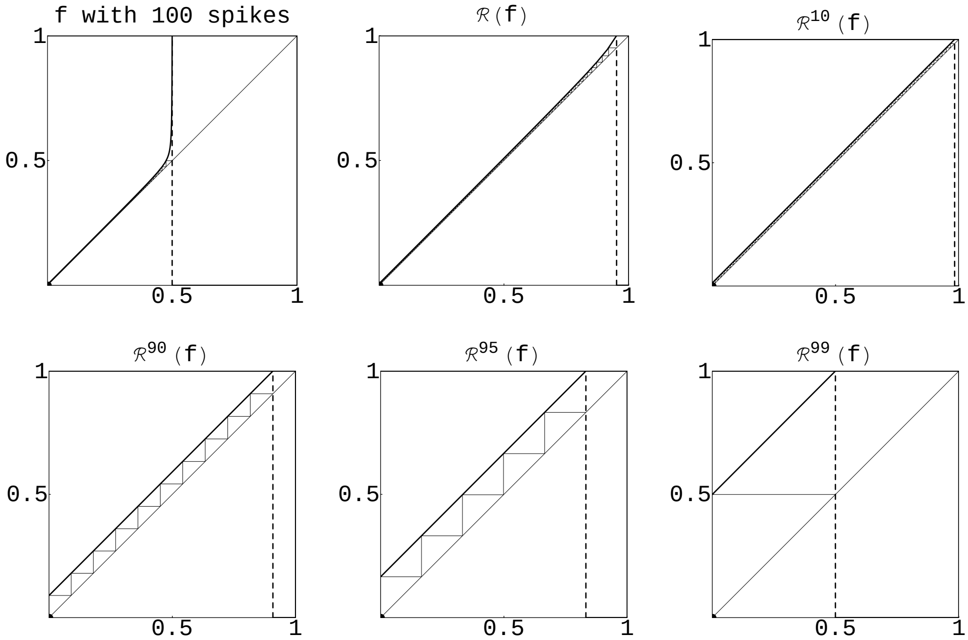

FIGURE 9. Same parameter values as in Fig.3 and $\varepsilon = \omega_{100}$. The saddle-effect of the fixed point $id = \psi_0$ is clear visible: $\mathcal{R}^k(f)$ moves closer to the fixed point ψ_0 before moving away from it. Also, $\mathcal{R}^{99}[f_{\omega_{100}}]$ is visually identical to $\psi_{1/2}$, another consequence to the saddle-effect.

Hence, there exists a sufficiently large K_0 so that for $k > K_0$ we have

$$\|\mathcal{R}^k[g_\mu] - \psi_{\mu_0}\| < \epsilon$$

for μ defined as in Eq.(5.7). Since $\mathcal{R}^k[g_\mu] = \mathcal{R}^{k+k_0}[f_\mu]$, the lemma is proved by choosing $N_0 = K_0 + k_0$. $\square$

Recall f_ε, the ε-parameter family of mapping (2.2) considered in the previous sections. Then the singular limit

$$f_0(x) = \lim_{\varepsilon\to 0} f_\varepsilon(x) = \begin{cases} x, & 0 \le x < .5 \\ 0, & .5 \le x \le 1 \end{cases} \in X$$

is attracted to ψ_0 because $\mathcal{R}[f_0] = \psi_0$. We believe the conditions of both the Universal Number 1 Theorem and the Inclination Lemma are satisfied and therefore both conclusions apply. The dynamical structure of $\mathcal{R}$ near ψ_0 as well as the family f_ε are depicted in Fig.8. A numerical simulation is shown in Fig.9 from which the saddle structure near the fixed point id and the inclination phenomenon are graphically demonstrated.

We end this subsection with some other backward invariant weakly expanding families through the fixed point $id = \psi_0$. They are similar to ψ_μ except with non-vanishing part over the right half interval. More specifically, consider families of the following form

$$g_{\mu,q}(x) = \begin{cases} x+\mu, & 0 \le x < 1-\mu \\ q_\mu(x), & 1-\mu \le x \le 1, \end{cases}$$

where $q_\mu(x) \ge 0$ and $\max_{[1-\mu,1]} q_\mu \le \mu$. It is straightforward to verify that the set $W^u_{id,q} := \{g_{\mu,q} : 0 \le \mu < 1/2\}$ is backward invariant if and only if

$$q_{\frac{\mu}{1-\mu}}(x) = \frac{1}{1-\mu} q_\mu((1-\mu)x+\mu), \frac{1-2\mu}{1-\mu} \le x \le 1.$$

For example, consider q_μ to be the logistic family $q_\mu = 4\lambda(x-1+\mu)(x-1)$. The x-intercepts are $x = 1-\mu = c_0$ and $x = 1$. The maximum takes place at $1-\mu/2$ with $\lambda\mu$ the maximum value. Because $g_{\mu,q}$ is linear on the left half interval $[0, c_0) = [0, 1-\mu)$, the renormalization $\mathcal{R}[g_{\mu,q}]$ on the right half interval $[(1-2\mu)/(1-\mu), 1]$ is again a quadratic function which goes through the zero at $x = (1-2\mu)/(1-\mu) = 1-\mu/(1-\mu)$ and $x = 1$ respectively and have the maximum value $\lambda\mu/(1-\mu)$ at $x = (1-\mu/2)/(1-\mu) = 1-\mu/[2(1-\mu)]$. It is precisely the quadratic function $q_{\mu/(1-\mu)}$. Thus, $W^u_{id,q}$ is backward invariant. One can construct other backward invariant families as well, e.g., replacing the logistic family by the tent map family gives rise to such a family. One can also show by the same argument as for Proposition 5.5 that such a backward invariant family is also tangent to u_0 at the fixed point $id = \psi_0$, i.e.,

$$\lim_{\mu\to 0} \frac{g_{\mu,q} - \psi_0}{\|g_{\mu,q} - \psi_0\|} = u_0,$$

where u_0 is the eigenvector of eigenvalue 1 as in Proposition 5.5. One can also show that if $\min_{x\in[c_0,1]} q_\mu(x) = 0$, then the same scaling laws as Proposition 5.6(c,d,e) hold for $g_{\mu,q}$ as well by exactly the same argument of that proposition. We note also that whether or not a mapping $g \in F[0,1]$ is isospiking has little to do with its dynamics on the interval $[0,1]$. For example, for the family $\{g_{\mu,q}\}$ with $q_\mu = 4\lambda(x-1+\mu)(x-1)$, its dynamics is determined by the logistic map. In fact, for $g_{\omega_n,q} \in \Sigma_n$, $\mathcal{R}^n[g_{\omega_n,q}](x) = \lambda x(1-x)$ is the logistic map. Also, for any fixed μ, the bifurcation diagram for $\{g_{\mu,q}\}$ with varying $\lambda \in (0,1)$ is essentially the diagram for the logistic family. Finally, we point out that for the neuron family f_ε of (2.2), $f_\varepsilon|_{[c(\varepsilon),1]}$ is of order $\exp(-1/\varepsilon)$. Thus, the dynamics of each mapping is very much regular. The $\exp(-1/\varepsilon)$ order estimate over its right interval results in the $\exp(-n)$ order estimate for the length of the nth nonisospiking interval.

5.2. **Superchaos.** We recall that

$$X = \{g \in Y : \exists x_* \in [0, c_0], \text{ s.t. } x_* = g(x_*^-)\}$$

where $g(x_*^-) = \lim_{x\to x_*^-} g(x)\}$. For $g \in X$, let $x_g = \sup\{x_* \in [0, c_0] : x_* = g(x_*^-)\}$. Then we also have $x_g = g(x_g^-)$. Define

$$X_0 = \{g \in X : x_g = 0\} \text{ and } X_1 = \{g \in X : x_g > 0\}.$$

Naturally we have $X = X_0 \cup X_1$.

Superchaos Theorem. (1) *For any $0 < \varrho < 1$, there is an element $s_\varrho \in X_1$ such that the orbit $\{\mathcal{R}^n[s_\varrho]\}$ converges to the fixed point $id = \psi_0$ at the rate of ϱ.*

(2) *For any $\varrho > 1$, there is a fixed point $r_\varrho \in X_0$ and a backward invariant family $U_\varrho \subset Y$ through r_ϱ on which $\mathcal{R}$ expands at the rate of ϱ.*

(3) *The set of periodic-n points of* $\mathcal{R}$ *in* X_0 *is infinite dimensional.*
(4) *The set of periodic points of* $\mathcal{R}$ *in* X_0 *is dense in* X_0.
(5) *The closure of the stable set of any* $h \in X_0$ *is* X_0. *More specifically, for any pair* $g \in X_0, h \in X_0$ *and any* $\epsilon > 0$, *there is an element* $f_{h,g} \in X_0$ *from the* ϵ-*neighborhood of* g, *i.e.,* $\|f_{h,g} - g\| < \epsilon$, *so that* $\mathcal{R}^n[f_{h,g}] = \mathcal{R}[h]$ *for some* $n \geq 0$.
(6) $\mathcal{R}$ *has the property of sensitive dependence on initial conditions. That is, there is a constant* $\delta_0 > 0$ *such that for any* $g \in X_0$ *and any small* $\epsilon > 0$, *there is an* $h \in X_0$ *and* $n > 0$ *satisfying* $\|h - g\| < \epsilon$ *and* $\|\mathcal{R}^n[h] - \mathcal{R}^n[g]\| \geq \delta_0$.
(7) *Any finite dimensional mapping is conjugate to* $\mathcal{R}$ *on a subset of* X_0 *and there are infinitely many such subsets of* X_0. *More precisely, for any finite dimensional mapping* $\theta : \mathbb{R}^n \to \mathbb{R}^n$, *there are infinitely many conjugate mappings* $\phi : \mathbb{R}^n \to X_0$ *such that* $\mathcal{R} \circ \phi = \phi \circ \theta$.
(8) *There is a dense orbit* $\{\mathcal{R}^n[g_*]\}_{n=0}^{\infty}$ *in* X_0.

Proof. 1) This is done by construction. For each $0 < \varrho < 1$, let

$$s_\varrho(x) = \begin{cases} x, & 0 \leq x \leq \dfrac{1}{2} \\[2ex] \dfrac{1}{\varrho}(x - \dfrac{1}{2}) + \dfrac{1}{2}, & \dfrac{1}{2} \leq x \leq \dfrac{1+\varrho}{2} \\[2ex] 0, & \dfrac{1+\varrho}{2} < x \leq 1. \end{cases}$$

Thus, we have $c_0 = (1+\varrho)/2$, and $x = 1/2$ is the largest fixed point of s_ϱ. Since s_ϱ is increasing with slope $1/\varrho$ in $[1/2, (1+\varrho)/2]$, $c_{-k} = s_\varrho^{-k}(c_0)$ exists for all k and $c_{-k} \searrow 1/2$ as $k \to \infty$. Also because s_ϱ is linear in $[1/2, (1+\varrho)/2]$, we have

$$\frac{1}{\varrho}\big(c_{-k} - c_{-(k+1)}\big) = (c_{-k+1} - c_{-k})$$

for all $k \geq 0$, with $c_0 = (1+\varrho)/2$ and extending the notation to $c_1 = 1$. Solving this equation gives

$$c_{-k} = \frac{1}{2}\big[\varrho^{k+1} + 1\big] \text{ for } k \geq 0 \text{ and } c_{-k} \to \frac{1}{2} \text{ as } k \to \infty.$$

By Proposition 5.2,

$$\mathcal{R}^k[s_\varrho](x) = \begin{cases} x, & 0 \leq x \leq \dfrac{1}{2c_{-k+1}} \\[2ex] \dfrac{1}{\varrho}(x - \dfrac{1}{2c_{-k+1}}) + \dfrac{1}{2c_{-k+1}}, & \dfrac{1}{2c_{-k+1}} \leq x \leq \dfrac{c_{-k}}{c_{-k+1}} \\[2ex] 0, & \dfrac{c_{-k}}{c_{-k+1}} < x \leq 1. \end{cases}$$

It is easy to see $\mathcal{R}^k[s_\varrho] \to id$ as $k \to \infty$. To demonstrate the convergence rate, we consider $\|\mathcal{R}^k[s_\varrho] - id\|$ which consists of calculating the area of the triangle between s_ϱ and the diagonal over the interval $[1/(2c_{-k+1}), c_{-k}/c_{-k+1}]$ and the trapezoid bounded between the diagonal and the x-axis over the interval $[c_{-k}/c_{-k+1}, 1]$.

Therefore,

$$\begin{aligned}\|\mathcal{R}^k[s_\varrho]-id\| &= \frac{1}{2}\big[\frac{c_{-k}}{c_{-k+1}}-\frac{1}{2c_{-k+1}}\big]\big[1-\frac{c_{-k}}{c_{-k+1}}\big]+\frac{1}{2}\big[1-\frac{c_{-k}}{c_{-k+1}}\big]\big[1+\frac{c_{-k}}{c_{-k+1}}\big]\\ &= \frac{1}{2}\frac{\varrho^k(1-\varrho)}{1+\varrho^k}\big[2\frac{c_{-k}}{c_{-k+1}}-\frac{1}{2c_{-k+1}}\big]\sim O(\varrho^k) \text{ as } k\to\infty.\end{aligned}$$

This proves statement 1).

Statement 2) is proved similarly. More precisely, for each $\varrho>1$, let r_ϱ be the fixed point which is the line of slope ϱ through the origin that is clipped at $c_0=1/\varrho$. That is,

$$r_\varrho(x)=\begin{cases}\varrho x, & 0\le x\le \dfrac{1}{\varrho}\\[2ex] 0, & \dfrac{1}{\varrho}<x\le 1.\end{cases}$$

Because of the linearity, r_ϱ is a fixed point of $\mathcal{R}$. Define U_μ as

$$U_\mu(x)=\begin{cases}\mu+\varrho x, & 0\le x\le \dfrac{1-\mu}{\varrho}\\[2ex] 0, & \dfrac{1-\mu}{\varrho}<x\le 1.\end{cases}$$

It is the same ray but translated upward by μ amount and clipped at $c_0=(1-\mu)/\varrho$. Again, since U_μ is linear in $[0,(1-\mu)/\varrho]$, U_μ is a backward invariant family with

$$\mathcal{R}[U_\mu]=U_{\frac{\varrho\mu}{1-\mu}}.$$

To show the statement, we only need to show that

$$\lim_{\mu\searrow 0}\frac{\|\mathcal{R}[U_\mu]-\mathcal{R}[U_0]\|}{\|U_\mu-U_0\|}=\varrho,$$

as we note that $U_0=r_\varrho$ and U_μ is a backward invariant family. The norm $\|U_\mu-U_0\|$ consists of the area of the parallelogram between U_μ and U_0 over the interval $[0,(1-\mu)/\varrho]$ and the area of the trapezoid between U_μ and U_0 over the interval $[(1-\mu)/\varrho,1/\varrho]$. We have

$$\begin{aligned}\|U_\mu-U_0\| &= \mu\frac{1-\mu}{\varrho}+\frac{1}{2}\big[\frac{1}{\varrho}-\frac{1-\mu}{\varrho}\big]\big[1+\varrho\frac{1-\mu}{\varrho}\big]\\ &= \frac{\mu}{\varrho}\big[2-\frac{3\mu}{2}\big].\end{aligned}$$

Therefore

$$\frac{\|\mathcal{R}[U_\mu]-\mathcal{R}[U_0]\|}{\|U_\mu-U_0\|}=\frac{\varrho}{1-\mu}\frac{2-\dfrac{3}{2}\dfrac{\varrho\mu}{1-\mu}}{2-\dfrac{3}{2}\mu}\to\varrho,\ \text{as } \mu\searrow 0.$$

This proves 2).

To show the rest statements 3)–8), we need to define a *concatenation* operation, denoted by $\bigvee$. Let g be any function over an interval $[c_{-k-1},c_0]\subset(0,1)$ with these properties: (i) $g(x)>x$ for $x\in[c_{-k-1},c_0]$; (ii) g is increasing; (iii) $g^{-k-1}(c_0)=c_{-k-1}$, i.e., $g(c_{-i})=c_{-i+1}$, $i=1,2,\dots,k+1$. Here we certainly assume c_{-i} depend on the individual function g. Let h be a function over $[d_1,d_0]\subset[0,1)$ such that

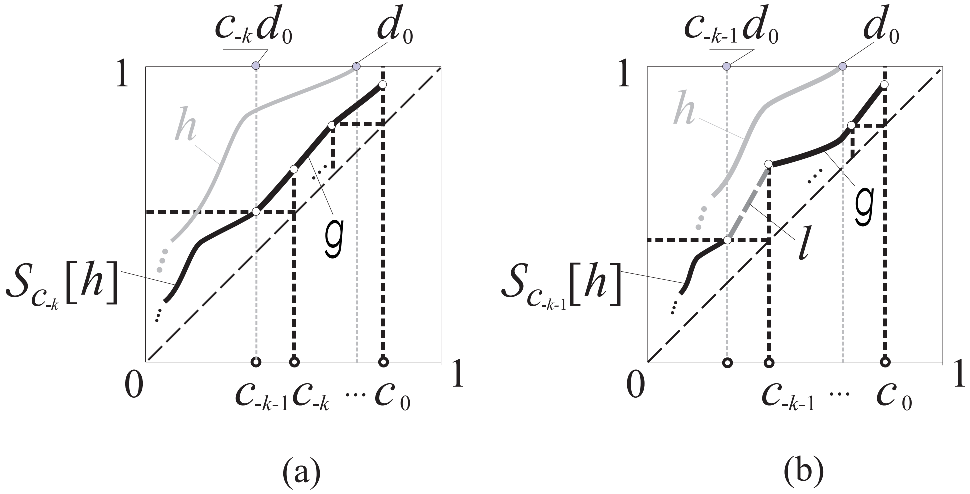

FIGURE 10. A schematic illustration for the definition of the concatenation operation $\bigvee$. (a) The case when $c_{-k}d_0 = c_{-k-1}$. (b) The other case when $c_{-k}d_0 \neq c_{-k-1}$.

$h(x) \geq x, x \in [d_1, d_0]$ and $h(d_0) = 1$. With a pair of such function g, h, we first scale down h by the factor of c_{-k}, and denote

$$\mathcal{S}_{c_{-k}}[h](x) = c_{-k}h(\frac{1}{c_{-k}}x),\ c_{-k}d_1 \leq x \leq c_{-k}d_0.$$

The operation $\bigvee$ is defined as follows. (a) If $c_{-k}d_0 = c_{-k-1}$, then we define

$$g \bigvee h(x) = \begin{cases} \mathcal{S}_{c_{-k}}[h](x), & c_{-k}d_1 \leq x \leq c_{-k}d_0 = c_{-k-1} \\ g(x), & c_{-k-1} \leq x \leq c_0, \end{cases}$$

see Fig.10(a). It is straightforward to check in this case that $g \bigvee h(x) \geq x$ and $g \bigvee h$ is continuous as $\mathcal{S}_{c_{-k}}[h](c_{-k-1}) = c_{-k}h(\frac{1}{c_{-k}}c_{-k}d_0) = c_{-k} \cdot 1 = g(c_{-k-1})$. (b) If $c_{-k}d_0 \neq c_{-k-1}$, then we consider

$$\mathcal{S}_{c_{-k-1}}[h](x) = c_{-k-1}h(\frac{1}{c_{-k-1}}x),\ c_{-k-1}d_1 \leq x \leq c_{-k-1}d_0 < c_{-k-1}.$$

Since $c_{-k-1}d_0 < c_{-k-1}$ the domains of $\mathcal{S}_{c_{-k-1}}[h]$ and g do not overlap. Also since $\mathcal{S}_{c_{-k-1}}[h](c_{-k-1}d_0) = c_{-k-1} < c_{-k} = g(c_{-k-1})$, $\mathcal{S}_{c_{-k-1}}[h]$ lies below $y = c_{-k}$ and g lies above $y = c_{-k}$. We define $g \bigvee h$ by joining the points $(c_{-k-1}d_0, c_{-k-1})$ and (c_{-k-1}, c_{-k}) in the box $[0,1] \times [0,1]$ by a line denoted by l. That is, we define

$$g \bigvee h(x) = \begin{cases} \mathcal{S}_{c_{-k-1}}[h](x), & c_{-k-1}d_1 \leq x \leq c_{-k-1}d_0 < c_{-k-1} \\ l(x), & c_{-k-1}d_0 \leq x \leq c_{-k-1} \\ g(x), & c_{-k-1} \leq x \leq c_0, \end{cases}$$

with

$$l(x) = \frac{c_{-k} - c_{-k-1}}{c_{-k-1} - c_{-k-1}d_0}(x - c_{-k-1}d_0) + c_{-k-1},$$

see Fig.10(b). Again, it is easy to see that $g \bigvee h$ is continuous and lies above the diagonal in this case as well. Other properties that are important for the rest of the proof are the following

- If h satisfies properties (i,ii,iii) as g does, then $g \bigvee h$ belongs to the same class as both g and h do.
- By definition, we already have $g \bigvee h(x) = g(x), x \in [c_{-k-1}, c_0]$. We also have
$$\mathcal{R}^i[g \bigvee h](x) = h(x) \text{ over } x \in [d_1, d_0]$$
for $i = k$ if $c_{-k}d_0 = c_{-k-1}$ and $i = k+1$ if $c_{-k}d_0 \neq c_{-k-1}$. Here we abuse the notation a little by treating $g \bigvee h$ as an element in X_0, which indeed can be the case by properly extending it to the rest of interval of $[0,1]$. This property is based on the fact that the scaling down operation $\mathcal{S}_c[h]$ and the scaling up operation $\mathcal{R}$ are inverse operations of each other.
- The operation is associative, i.e., $g \bigvee (h \bigvee f) = (g \bigvee h) \bigvee f$. Thus, we denote
$$g \bigvee h \bigvee f = g \bigvee (h \bigvee f).$$
- If all defined, we use the following notation
$$\bigvee_{i=1}^{\infty} g_i = \lim_{n\to\infty} \bigvee_{i=1}^{n} g_i = g_1 \bigvee g_2 \bigvee g_3 \cdots .$$
Also, we will use the fact that the limit $\lim_{x\to 0^+} \bigvee_{i=1}^{\infty} g(x) = 0$ exists and equals 0. In fact, we note that for any $n \geq 1$, the function $\bigvee_{i=1}^{n} g$ is defined over an interval $[a_n, c_0]$ whose left end point a_n is bounded from above by $c_{-k-1}c_{-k}^{n-1}$ by the definition of $\bigvee$. Thus, $a_n \to 0$ as $n \to \infty$ and $\lim_{x\to 0^+} \bigvee_{i=1}^{\infty} g_i(x) = 0$ follows by the monotonicity of the infinite concatenation.

We are now ready to show 3). Let $\varrho > 1$ be any fixed number and consider the fixed point $r_\varrho(x) = \varrho x, 0 \leq x \leq 1/\varrho$ and $r_\varrho = 0, x > 1/\varrho$ that was considered in the proof of statement 2). Let $c_0 = 1/\varrho$. Then by the linearity of r_ϱ over $[0, c_0]$, we have $c_{-k} = 1/\varrho^{k+1}$. For any fixed natural number $n \geq 1$, let $h_1, h_2, \ldots, h_n$ be n distinct increasing functions over $[c_{-1}, c_0]$ such that for all $i = 1, 2, \ldots, n$ we have $h_i(x) > x, x \in [c_{-1}, c_0]$, $h_i(c_{-1}) = c_0$, and $h_i(c_0) = 1$. We construct $h = \bigvee_{i=1}^{n} h_i(x)$ and then concatenate h indefinitely to get

$$p_n(x) = \begin{cases} \bigvee_{j=1}^{\infty} h = \bigvee_{j=1}^{\infty} \bigvee_{i=1}^{n} h_i(x), & 0 < x \leq c_0 \\ 0, & \text{either } x = 0 \text{ or } c_0 < x \leq 1, \end{cases}$$

It is straightforward to verify that $p_n \in X_0$ and $\mathcal{R}^n[p_n] = \bigvee_{i=2}^{\infty} h = p_n$ but $\mathcal{R}^k[p_n] \neq p_n$ for $1 \leq k < n$. So p_n is a period-n point of $\mathcal{R}$ in X_0. Because h_i are arbitrary functions with the described properties, the set of period-n points is infinite dimensional. This proves statement 3).

To show statement 4), we need to show that for any $g \in X_0$, we can find a sequence of periodic points p_k such that $p_k \to g$ as $k \to \infty$. To construct p_k, we begin with the fact that since $g(x) > x$ for $0 < x \leq c_0$, $g(0) = 0$, and g is increasing in $[0,c_0]$, thus $c_{-k}=g^{-k}(c_0)$ must exists for all $k\geq 1$ and $c_{-k}\to 0$ as $k\to\infty$. If $g(c_0)=1$, then we let $\tilde{g}_k=g|_{[c_{-k-1},c_0]}$. If $g(c_0)<1$, then for large k we let

$$\tilde{g}_k(x)=\begin{cases} g(x), & c_{-k-1}\leq x\leq c_0-\frac{1}{k}\\ k[1-g(c_0-\frac{1}{k})](x-c_0)+1, & c_0-\frac{1}{k}\leq x\leq c_0.\end{cases}$$

That is, $\tilde{g}_k$ in this case is constructed to be g over $[0,c_0-1/k]$ and the line connecting the point $(c_0-1/k, g(c_0-1/k))$ on the graph of g and the point $(c_0,1)$ on the top edge of the box $[0,1]\times[0,1]$. In both cases $\tilde{g}_k$ satisfies the conditions (i,ii,iii) for the concatenation operation $\bigvee$. Hence, if we let

$$p_k(x)=\begin{cases} \bigvee_{i=1}^{\infty}\tilde{g}_k(x), & 0<x\leq c_0\\ 0, & x=0 \text{ or } c_0<x\leq 1,\end{cases}$$

then we see p_k is continuous at $x=0$ by the last property we listed above after the definition of $\bigvee$. Moreover, $p_k\in X_0$ and either $\mathcal{R}^k[p_k]=p_k$ or $\mathcal{R}^{k+1}[p_k]=p_k$, depending on whether or not $c_{-k}c_0=c_{-k-1}$. Thus, p_k is a periodic point of $\mathcal{R}$. Since p_k and g differ only on $[0,c_{-k}]$ and possibly on $[c_0-1/k,c_0]$, we have

$$\|p_k-g\|=O(\max\{\frac{1}{k},c_{-k}\})\to 0 \text{ as } k\to\infty.$$

This proves statement 4).

To show 5), let $g\in X_0$ and $h\in X_0$. As in the proof of 4) above, $c_{-k}=g^{-k}(c_0^g)\to 0$ as $k\to\infty$. Let $g_k=g|_{[c_{-k-1},1]}$. Then g_k and $\mathcal{R}[h]$ satisfy the conditions for the concatenation operation $\bigvee$, and we define $f_{h,g}=g_k\bigvee\mathcal{R}[h]$. Clearly $f_{h,g}\in X_0$. Since $f_{h,g}$ and g differ only possibly on $[0,c_{-k-1}]$, we have $\|f_{h,g}-g\|=O(c_{-k-1})$. Also, by a property of $\bigvee$, either $\mathcal{R}^k[f_{h,g}]=\mathcal{R}[h]$ or $\mathcal{R}^{k+1}[f_{h,g}]=\mathcal{R}[h]$ depending on whether or not $c_{-k}c_0^h=c_{-k-1}$. Thus, for any $\epsilon>0$, there is an integer $n\geq 1$ so that $\|f_{h,g}-g\|<\epsilon$ and $\mathcal{R}^n[f_{h,g}]=\mathcal{R}[h]$. This proves statement 5).

To show 6), we need to construct an $h\in X_0$ for each $g\in X_0$ that satisfies the stated properties. To this end, we first demonstrate that any $g\in X_0$ can be properly separated from some element $\ell\in X_0$ by construction. More specifically, let $c_0\in[0,1]$ be the point of discontinuity of g. Then there is always a point in $(0,1)$ denoted by c_0^ℓ that is no less than $1/4$ apart from c_0:

$$|c_0^\ell-c_0|\geq\frac{1}{4}.$$

Let ℓ be the line through the origin $(0,0)$ and $(c_0^\ell,1)$ over $[0,c_0^\ell]$ and 0 over $(c_0^\ell,1]$. Then $\|\ell-g\|$ must be greater than the area of the trapezoid below the diagonal and over the interval $[c_0^\ell,c_0]$ if $c_0^\ell<c_0$ and $[c_0,c_0^\ell]$ if $c_0<c_0^\ell$. This area is in turn greater than the area of the equal lateral right triangle which is the top part of the trapezoid. Since the area of that triangle is

$$\frac{1}{2}|c_0^\ell-c_0||c_0^\ell-c_0|\geq\frac{1}{2}\times\frac{1}{4}\times\frac{1}{4}=\frac{1}{32}:=\delta_0,$$

it follows that

$$\|\ell-g\|>\delta_0=\frac{1}{32}.$$

We are now ready to show the property of sensitive dependence on initial conditions. For each $g\in X_0$, we have $c_{-k}=g^{-k}(c_0)\to 0$ as $k\to\infty$. For each k, let ℓ_k be such a function associated with $\mathcal{R}^{k+1}[g]$ that is separated from $\mathcal{R}^{k+1}[g]$ by at

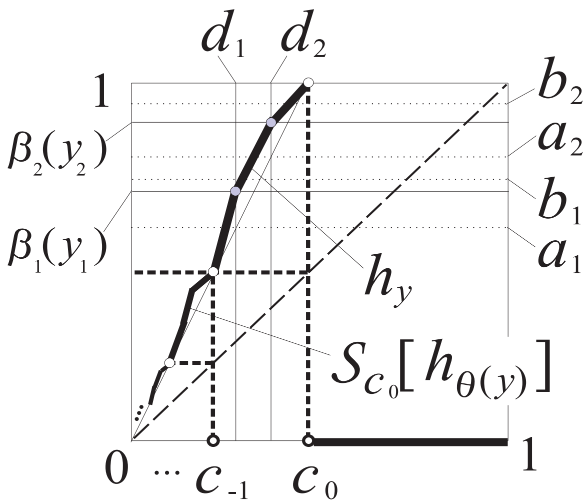

FIGURE 11. A schematic illustration for conjugating a 2-dimensional map $\theta : \mathbb{R}^2 \to \mathbb{R}^2$ to a sub-dynamics of $\mathcal{R}$.

least δ_0 amount. Moreover, we impose the condition that $c_0^{\ell_k} c_{-k} \neq c_{-k-1}$ in the construction of ℓ_k. Let $g_k = g|_{[c_{-k-1},1]}$ and define

$$h_k = g_k \bigvee \ell_k.$$

It is obvious that $\|h_k - g\| \leq c_{-k-1} \to 0$ since h_k and g differ only in the interval $[0, c_{-k-1}]$ with $h_k|_{[c_{-k-1},1]} = g_k = g|_{[c_{-k-1},1]}$. However, because $c_0^{\ell_k} c_{-k} \neq c_{-k-1}$, we have by the definition of $\bigvee$ that

$$\|\mathcal{R}^{k+1}[h_k] - \mathcal{R}^{k+1}[g]\| = \|\ell_k - \mathcal{R}^{k+1}[g]\| > \delta_0.$$

This proves 6).

To show 7) we need to construct a conjugacy ϕ for each mapping $\theta : \mathbb{R}^n \to \mathbb{R}^n$ that maps any point $y \in \mathbb{R}^n$ to a corresponding element $\phi(y) \in X_0$ so that $\mathcal{R} \circ \phi(y) = \phi \circ \theta(y)$. The construction to be used below will shows that there are infinitely many such ϕ for every mapping θ.

We start by fixing any $\varrho > 1$ and the ray r_ϱ considered in the proof of statement 2) above. Here $r_\varrho(x) = \varrho x, 0 \leq x < 1/\varrho$ and $r_\varrho(x) = 0, 1/\varrho < x \leq 1$. The point of discontinuity is $c_0 = 1/\varrho$ and $c_{-k} = 1/\varrho^{k+1}$ with $r^{-1}(c_{-k}) = c_{-k-1}, k = 0, 1, 2, \ldots$. The goal is to construct for each $y \in \mathbb{R}^n$ an element $g = \phi(y) \in X_0$ with the property that $c_{-k}^g = c_{-k} = 1/\varrho^{k+1}, k = 0, 1, 2, \ldots,$ and $\mathcal{R} \circ \phi(y) = \mathcal{R}[g](y) = \phi \circ \theta(y)$, see Fig.11. In fact, we will construct g to be a piecewise linear curve from X_0 having exactly $n+1$ line segments over each interval $[c_{-k-1}, c_{-k}], k = 0, 1, 2, \ldots$. The key step is in constructing the piece over the first interval $[c_{-1}, c_0]$ by embedding $\mathbb{R}^n$ into the space of piecewise linear functions from $[c_{-1}, c_0]$ to $[c_0, 1]$.

To this end, we first arbitrarily pick and fix n points $c_{-1} < d_1 < d_2 < \cdots < d_n < c_0$. Denote the images of d_i under r_ϱ by $a_i = r_\varrho(d_i) = \varrho d_i, 1 \leq i \leq n$. By r_ϱ's monotonicity, this gives $c_0 = r_\varrho(c_{-1}) < a_1 < a_2 < \cdots < a_n < 1 = r_\varrho(c_0)$. We then arbitrarily pick and fix b_i so that $a_i < b_i < a_{i+1}, i = 1, 2, \ldots, n$ with

$a_{n+1} = 1$. We are now ready to embed $\mathbb{R}^n$ into the space of piecewise linear functions from $[c_{-1}, c_0]$ to $[c_0, 1]$. More specifically, let $\beta_i : \mathbb{R} \to (a_i, b_i)$ be any 1-to-1 and onto map and let $y = (y_1, y_2, \ldots, y_n) \in \mathbb{R}^n$ with y_i being the ith coordinate. We then define h_y to be the graph over interval $[c_{-1}, c_0]$ that connects the vertex points $(c_{-1}, c_0), (d_1, \beta_1(y_1)), \ldots, (d_i, \beta_i(y_i)), \ldots, (d_n, \beta_n(y_n))$, and $(c_0, 1)$ with line segments. Because of the choice that $\beta_i(y_i) < b_i < a_{i+1} < \beta_{i+1}(y_{i+1})$, each line through $(d_i, \beta_i(y_i))$ and $(d_{i+1}, \beta_{i+1}(y_{i+1}))$ must be increasing. Hence h_y is increasing in $[c_{-1}, c_0]$. It is continuous by construction and $h_y(c_{-1}) = c_0, h_y(c_0) = 1$. It lies above the diagonal because it lies above the ray r_ϱ. Therefore $h_y \bigvee h_z$ is well-defined with any $y, z \in \mathbb{R}^n$, in particular, with $z = \theta(y)$. We now complete our construction for $g = \phi(y)$ by defining

$$g = \phi(y) = \begin{cases} \bigvee_{i=0}^{\infty} h_{\theta^i(y)}(x), & 0 < x \le c_0 \\ 0, & x = 0 \text{ or } c_0 < x \le 1, \end{cases}$$

see Fig.11. By the definition of $\bigvee$ we have $\mathcal{R}[\phi(y)](x) = \bigvee_{i=1}^{\infty} h_{\theta^i(y)}(x) = \phi(\theta(y))(x)$ for $x \in [0, c_0)$ and 0 otherwise. That is, $\mathcal{R}[\phi(y)] = \phi(\theta(y))$ as desired. Finally, we point out that there are infinitely many ways to construct the conjugacy ϕ above by, e.g., starting with distinct rays r_ϱ for $\varrho > 1$, or by varying the parameters d_i, a_i, b_i. This proves 7). (Also, it is easy to see by the construction above that this result can be generalized to include mappings on product spaces, e.g., $\mathbb{R}^\omega$, which include shift maps.)

The proof of statement 8) is based on the fact that the $L^1[0,1]$ space is separable, i.e., having a countable dense set. To be precise, let $\mathcal{D}_1$ denote the subset of $L^1[0,1]$ that contains piecewise continuous and piecewise-linear functions connecting vertexes of rational coordinates, in particular, with vertexes having the x-coordinates in the form of i/n for $0 \le i \le n$ and $n \ge 2$. Clearly $\mathcal{D}_1$ is countable and dense. For each $g \in X_0$, we can certainly approximate it by a sequence of functions g_n from $\mathcal{D}_1$ each of which is i) continuously increasing over $[0, c_0^{g_n}]$, i.e., $g_n(x_1) < g_n(x_2), 0 \le x_1 < x_2 \le c_0^{g_n}$; ii) above the diagonal $y = x$ over $[0, c_0^{g_n}]$, i.e., $g_n(x) > x, 0 < x \le c_0^{g_n}$; iii) vanishing at 0 and in $(c_0^{g_n}, 1]$. In other words, such a sequence can come from X_0. That is, X_0 itself is separable with the countable dense set $\mathcal{D}_2 = X_0 \cap \mathcal{D}_1$. Next for each $g \in \mathcal{D}_2$ we modify it to get a sequence by taking the following two steps. (1) If $g(c_0^g) = 1$, we do nothing about the discontinuity point c_0^g and set $g_n = g$. (2) Otherwise, $g(c_0^g) < 1$. Then we construct a sequence g_n with i) $c_0^{g_n} = c_0^g + 1/n$; ii) $g_n(x) = g(x)$ for $0 \le x \le c_0^g$ and $c_0^g + 1/n < x \le 1$; iii) g_n is the line connecting $(c_0^g, g(c_0^g))$ and $(c_0^{g_n}, 1)$. It is trivial to see that $g_n \in \mathcal{D}_2$ and $g_n \to g$ in L^1. That is, g_n is everything of any other $\mathcal{D}_2$ elements except that $g_n(c_0^{g_n}) = 1$. Denote this subset of $\mathcal{D}_2$ by $\mathcal{D}_3 \subset \mathcal{D}_2 \subset X_0$. Then we know $\mathcal{D}_3$ is countable and dense in $\mathcal{D}_2$, so is dense in X_0. We further modify $\mathcal{D}_3$ as follows. For each $g \in \mathcal{D}_3$, we have $c_{-k} = g^{-k}(c_0) \to 0$ as $k \to \infty$ as $x = 0$ is the only fixed point of g. We construct a sequence h_k each is the function g restricted on $[c_{-k}, c_0]$, i.e., $h_k = g|_{[c_{-k}, c_0]}$. This sequence $\{h_k\}$ has the property that by making any L^1-extension of h_k to the left-over interval $[0, c_{-k}]$, we will always have

$$\|h_k - g\|_{L^1[0,c_0]} \le c_{-k} \to 0 \text{ as } k \to \infty.$$

Denote by $\mathcal{D}_4$ the set of all $h_k = g|_{[c_{-k}, c_0]}$ for all $g \in \mathcal{D}_3$. Then $\mathcal{D}_4$ is a countable set. Also, although $\mathcal{D}_4$ is not a subset of X_0, it can be treated to be dense in X_0 because for each $g \in X_0$ there is a sequence $\{g_{n_k}\}$ from $\mathcal{D}_4$ such that with an arbitrary extension to $[0, a_k]$ and 0 to $[c_0^{g_{n_k}}, 1]$ for each g_{n_k} with $[a_k, c_0^{g_{n_k}}]$ the domain of g_{n_k}, we have $g_{n_k} \to g$ as $k \to \infty$.

We are now ready to construct a dense orbit in X_0. Since $\mathcal{D}_4$ is countable, we have

$$\mathcal{D}_4 = \{g_1, g_2, \ldots, \}.$$

We now construct

$$g_* = \begin{cases} \bigvee_{i=1}^{\infty} g_i(x), & 0 < x \le c_0^{g_1} \\ 0, & x = 0 \text{ or } c_0^{g_1} < x \le 1. \end{cases}$$

It is obvious that by the definition of the concatenation operation $\bigvee$, g_* is continuous and increasing over the left open interval $(0, c_0^{g_1})$. Let $c_0 = c_0^{g_*}$ and $c_{-k} = g_*^{-k}(c_0)$. It is obvious that $c_{-k} \in [0, c_0)$ exist for all $k \ge 0$ by the definition of infinite concatenation as in $\bigvee_{i=1}^{\infty} g_i$. Therefore, $c_{-k} \searrow x_*$ exists as $k \to \infty$ and $x_* \in [0, c_0)$ is a fixed point of g_*. To show g_* is continuous at $x = 0$ and $g_* \in X_0$, we only need to show that $x_* = 0$. Suppose otherwise that $x_* > 0$. Then, $g_0 = \lim_{k\to\infty} \mathcal{R}^k[g_*]$ must exist and g_0 is a fixed point of $\mathcal{R}$ with $g_0(1^-) = 1$. On the other hand, by the definition of $\bigvee$ we have $g_n(x) = \mathcal{R}^k[g_*](x)$ for some $k \ge 0$, with k depending on n, and for all x from g_n's domain of definition $[a_n, c_0^{g_n}]$. The existence of the limit $g_0 = \lim_{k\to\infty} \mathcal{R}^k[g_*]$ forces the conclusion that $c_0^{g_n} \to 1$ as $n \to \infty$. Since $\mathcal{D}_4 = \{g_n\}$ can be regarded as a dense set of X_0, the existence of the limit $c_0^{g_n} \to 1$ would imply that every element $g \in X_0$ must have the property that $g(1^-) = 1$. This is certainly a contradiction to the fact that $x = 0$ is the only fixed point for every element $g \in X_0$. This completes the proof that $g_* \in X_0$.

We are now ready to show that the orbit through g_* is dense in X_0. In fact, for any $g \in X_0$ and any $\epsilon > 0$, there is a $g_k \in \mathcal{D}_4$ that is ϵ-close to g with any arbitrary X_0-extension of g_k to the left of its domain and 0 extension to the right of its domain. By the definition of the concatenation operation $\bigvee$ there is an integer n such $\mathcal{R}^n[g_*] = g_k \bigvee \bigvee_{i=k+1}^{\infty} g_i$ over $[0, c_0^{g_k}]$ and 0 over $[c_0^{g_k}, 1]$. Hence, $\mathcal{R}^n[g_*]$ is ϵ-close to g. This shows that the orbit $\{\mathcal{R}^n[g_*]\}$ is dense in X_0. □

We end this section by pointing out the structure of X_1 is completely understood. In fact for every $g \in X_1$, there is a non-vanishing left fixed point $g(x_*^-) = x_* > 0$. From the proof above we know that the limit $h = \lim_{k\to\infty} \mathcal{R}^k[g]$ exists and it is a fixed point of $\mathcal{R}$ for which $x = 1$ is a fixed point of h. Also, it is straightforward to show that an element from the stable set of such a fixed point h must be in X_1. Therefore, we can conclude the following.

Proposition 5.8. *X_1 consists all fixed points h of $\mathcal{R}$ satisfying $h(1) = 1$ and all their stable sets.*

6. Summary

We started with one hypothesis that the per-burst spike number of excitable cells is coded information in a possible encoding scheme for neuron-to-neuron communications. We derived a one-parameter family of interval mappings f_ε, phenomenologically modeling the bursting-spiking behaviours of excitable cells, which include pancreatic β-cells. We derived bifurcation criterion for the model map to be isospiking. Scaling laws governing the isospiking intervals were obtained. A new renormalization operator $\mathcal{R}$ was used to explain these scaling laws. By this approach, the phenomenological family presents a curve in the renormalization space Y that ends on the stable set X of the renormalization fixed point ψ_0 at $\varepsilon = 0$. From this renormalization point of views, other excitable and neuron cell models, conceivably, and more importantly, the physiological kind, can be treated as elements or curves in the renormalization space Y. As such they must obey the same universality laws as the phenomenological family does. This is the value and justification to use our phenomenological model for excitable cell modeling. Based on the neuroencode hypothesis, we discovered that the first natural number 1 is a universal constant, in a similar sense as Feigenbaum's. We also discovered that every finite dimensional systems can be conjugate to a sub-system of the renormalization operator $\mathcal{R}$ in a subset X_0 of the stable set X of ψ_0, and the conjugation can be done in infinitely many ways. Also, we showed that there is an orbit from X_0 that is dense in X_0. It is rather interesting that these three elements — neuroencode hypothesis, universal number 1, superchaos — come together in one renormalization paradigm. Each separate from the others would be less so.

Appendix A. Further Justification of the Return Map (2.2)

The slow subsystem of Eq.(2.1) with $\varsigma = 0$ is a 2-dimensional system restricted on the nullcline of the faster variable n:

$$0 = (n - n_{\min})(n_{\max} - n)[(V - V_{\max}) + r_1(n - n_{\min})] - \eta_1(n - r_2).$$

For $\eta_1 = 0$, it consists of three planes $n = n_{\min}$, $n = n_{\max}$, and $V = V_{\max} + r_1(n - n_{\min})$. For $\eta_1 > 0$, these planes are perturbed to become three disjoint surfaces of which only the Z-shaped hysteresis surface, referred to as the Z-switch, is relevant to our consideration, see Fig.12(a). Divide the switch into three branches: the front branch $\mathcal{S}_1$, the middle branch $\mathcal{S}_3$, and the back branch $\mathcal{S}_2$ as in Fig.2 and Fig.12(a). Both $\mathcal{S}_1$ and $\mathcal{S}_2$ consist of stable equilibrium points for the faster n-equation and the middle branch $\mathcal{S}_3$ unstable points. The common boundary $\mathcal{T}_1$ of $\mathcal{S}_1$ and $\mathcal{S}_3$, and $\mathcal{T}_2$ of $\mathcal{S}_2$ and $\mathcal{S}_3$ respectively are the turning points of the Z-switch, or saddle-node bifurcation points of the faster n-equation when C and V are viewed as parameters. At the limit $\eta_1 = 0$, $\mathcal{S}_1$ and $\mathcal{S}_2$ become half planes given by $n = n_{\min}, V < V_{\max}$ and $n = n_{\max}, V > V_{\rm spk}$, respectively. The middle branch becomes a planar section. Also for $\eta_1 = 0$, the turning edges $\mathcal{T}_1 = \{n = n_{\min}, V = V_{\max}\}$ and $\mathcal{T}_2 = \{n = n_{\max}, V = V_{\rm spk}\}$ are lines. For a simpler presentation, we will treat the perturbed Z-switch with $\eta_1 > 0$ the same as the unperturbed one with $\eta_1 = 0$. In this way, all the components $\mathcal{S}_i$ and $\mathcal{T}_j$ are linear objects and many notations introduced below will be greatly simplified. For this simplification to work, we only need to assume that the turning edges $\mathcal{T}_j$ do not touch any other part of the n-equilibrium set, i.e., there are small openings near $\mathcal{T}_i$ so that all the faster n-solutions immediately above $\mathcal{T}_1$ are attracted to the back branch $\mathcal{S}_2$ and those immediately below $\mathcal{T}_2$ are attracted to the front branch $\mathcal{S}_1$ respectively. It is important to note that this simplification does not affect the return map defined in (2.2).

To motivate the definition, we now describe some essential phase portrait feature for the reduced CV dynamics on the Z-switch. On $\mathcal{S}_1$, Eq.(2.1) with our simplistic assumption $\eta_1 = 0$ becomes

$$\dot{C} = \varepsilon(V - \varrho)$$
$$\dot{V} = (n_{\max} - n_{\min})[(V - V_{\min})(V - V_{\min} - r_3(C - C_{\min})) + \eta_2],$$

which is a singularly perturbed system with $0 < \varepsilon \ll 1$. The V-nullcline

$$0 = (n_{\max} - n_{\min})[(V - V_{\min})(V - V_{\min} - r_3(C - C_{\min})) + \eta_2]$$

consists of two lines $V = V_{\min}$ and $V = V_{\min} + r_3(C - C_{\min})$ for $\eta_2 = 0$. For $\eta_2 > 0$, it splits into two disjoint V-shaped curves pointed sideways, see Fig.12(b). We will ignore the left one and restrict our model to the right half plane of a vertical line which separates the two curves. We will refer to the right half of the V-nullcline the V-nullcline for simplicity. Equilibrium points of the horizontal branch of the V-nullcline are asymptotically stable and those of the diagonal branch are unstable. The knee point is a saddle-node bifurcation point of the V-equation when C is viewed as a parameter with $\varepsilon = 0$. The C-nullcline is $V = \varrho$ which intersects the V-nullcline at a unique point (C_*, ϱ) for $V_{\min} < \varrho < V_{\max}$, where $C_* \to C_{\rm cpt}$ as $\eta_2 \to 0$. For a more transparent presentation, we will simply set $C_* = C_{\rm cpt}$ by assuming that the part of the V-nullcline that intersects the C-nullcline remains unchanged for all small $\eta_2 \geq 0$. For $\varepsilon > 0$, $(C_{\rm cpt}, \varrho)$ is the only equilibrium point of the CV-system and it is a source. All nonstationary solutions converge to the source backward in time and more importantly, they all escape the surface $\mathcal{S}_1$ through the turning edged $\mathcal{T}_1$. More specifically, let Γ^* denote the orbit through the point labeled as p^* in Fig.2. Unlike all other $\mathcal{T}_1$ turning points, p^* is the only point at which the CV-vector field is tangent to $\mathcal{T}_1$. Also, let Γ_* be the orbit through the knee point of the V-nullcline. Then for sufficiently small $\varepsilon > 0$, all nonstationary solutions started below $\Gamma_* \cup \Gamma^*$ will be first attracted to the horizontal branch of the V-nullcline, only to evolve slowly along the branch in the decreasing C-direction before clearing the knee point and heading upward to the turning edge $V = V_{\max}$. The fate for other nonstationary solutions is the same. Note that they all escape through the half line of $\mathcal{T}_1$ left to the tangential turning point p^*.

When restricted to $\mathcal{S}_2$, the reduced CV-dynamics is relatively simple:

$$\dot{C} = \varepsilon(V - \varrho), \qquad \dot{V} = -w(n_{\max} - n_{\min}).$$

That is, $V_{\rm spk} \in (V_{\min}, V_{\max})$ is the lower bound of the V-component, and every solution on $\mathcal{S}_2$ escapes through the turning edge $\mathcal{T}_2 = \{V = V_{\rm spk}\}$ in a finite time. For simplification, we will assume that $w > 0$ is infinity so that solutions on $\mathcal{S}_2$ reach the turning edge $\mathcal{T}_2$ instantaneously in the fast V direction. In this way, we will only use the essential role of the $\mathcal{S}_2$-dynamics that it takes points downward to the turning edge $\mathcal{T}_2$, keeping other complications of $\mathcal{S}_2$ to minimum in defining the return map. This simplification again does not affect the map in any significant way.

We begin by fixing the domain and range of definition. They are completely determined by the tangential turning point p^* and here is why. Unlike transversal turning points, there are two ways to start an orbit from p^*. One way follows the CV-orbit on $\mathcal{S}_1$ first and continues on in the manner of defining the return map until it hits $\mathcal{J}_1$, i.e., the concactation orbit has to hit $\mathcal{J}_1$ from $\mathcal{T}_2$. The junction point is labeled as $R_{\min}$ in Fig.2 and we set $R_{\min} \Rightarrow 0$, the left end point of the map's domain. The other way to associate an orbit with p^* is to follow the faster n-flow to $\mathcal{S}_2$ and then return to $\mathcal{J}_1$. The junction point is labeled as $R_{\max}$ in Fig.2. Note

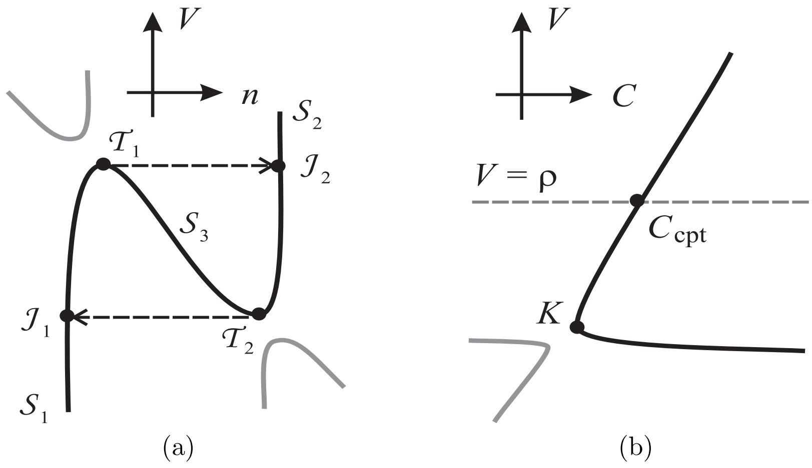

FIGURE 12. (a) The nV-cross section view of the Z-switch for $\eta_1 > 0$. (b) For $\eta_2 > 0$, the nullcline for variable V consists of two V-shaped curves. All light colored nullclines are outside a neighborhood for the bursting-spiking region, thus can be dropped from consideration.

that by our assumption on $\mathcal{S}_2$, $R_{\max}$ is directly below p^*. We set it to $R_{\max} \Rightarrow 1$, the right end point of domain. We set $C_{\rm cpt} \Rightarrow .5$, the middle point of the domain.

We now explain why Π maps $[0,1]$ into itself. We start with the end points. For the case of $R_{\min}$, the return point must lie above $R_{\min}$ because $\dot{C} = \varepsilon(V - \varrho) > 0$ for $V(t) \geq V_{\rm spk} > \varrho$. Also, observe that the return map is monotone increasing on the interval $[R_{\min}, c)$ and its left limit at c is $R_{\max}$. These facts combined imply $R_{\min}$ is mapped into $(R_{\min}, R_{\max})$. For the case of $R_{\max}$, the point is directly below p^* and $R_{\min}$'s defining CV-orbit Γ^* through p^* is horizontal, implying the first intersection P (not return!) of Γ^* with $\mathcal{J}_1$ must be above $R_{\max}$. Because the orientation of the interval $[R_{\max}, P]$ is reversed by the CV-flow when first intersecting the half of $\mathcal{J}_1$ left to c and then preserved afterwards when hitting $\mathcal{J}_1$ from $\mathcal{T}_2$, we must have $R_{\min} = \Pi(P) < \Pi(R_{\max}) < R_{\max}$. To explain Π maps the entire interval $[R_{\min}, R_{\max}]$ into itself, we only need do so for the three subintervals partitioned by points c and $C_{\rm cpt}$. We already demonstrated the case with $[R_{\min}, c)$ above. The case with $[C_{\rm cpt}, R_{\max}]$ follows the same argument as for $[R_{\max}, P]$. In fact, Π is monotone decreasing on $[C_{\rm cpt}, R_{\max}]$. As for the case with $[c, C_{\rm cpt})$, the interval is first taken by the CV-flow onto $(C_{\rm cpt}, R_{\max}]$, reversing its orientation, and then taken by the action of Π on $[C_{\rm cpt}, R_{\max}]$, reversing its orientation back again. Therefore, Π is monotone increasing on $[c, C_{\rm cpt})$, mapping c to $R_{\min}$.

Analytical forms more accurate than (2.2) exist for Π. However they must all satisfy the properties (2.3–2.5) and those we now describe.

The termination point c must coincide with $C_{\rm cpt} = .5$ when either $\varepsilon = 0$ or $\varrho = 0$. The order estimate for c in ε and ϱ could be actually higher than linear as assumed in (2.2) but a more accurate estimate matters little to our analysis.

As for the left limit at point c, Π must map a small neighborhood left to c to a greater portion of the right half interval $[.5, 1]$ and the graph of Π must be asymptotically tangent to the vertical line through c. This can be seen by a simplistic argument as follows. Assume the CV-flows on $n = n_{\min}$ are a collection of parabola-like curves near p^* and are given as

$$V = -|C - p^*|^\sigma + V_{\max} + q, \text{ with } C < p^*,$$

where $\sigma > 1$ and $q \geq 0$ parameterizes the collection with $q = 0$ corresponding to the curve tangent to $V = V_{\max}$ at p^*. Let C_0 and C_1 be points on the curve with a given q so that $V(C_0) = V_{\rm spk}$ and $V(C_1) = V_{\max}$. Then we can solve explicitly as

$$(C_0 - p^*)^\sigma - V_{\max} = q, C_1 = p^* + q^{1/\sigma}.$$

Differentiating C_1 in C_0 gives

$$\frac{dC_1}{dC_0} = q^{(1/\sigma)-1}(p^* - C_0)^{\sigma-1}$$

which goes to infinity at the point C_0 for which $q = 0$ and $(p^* - C_0) = V_{\max}^{1/\sigma}$. The order of divergence is $q^{(1/\sigma)-1}$. This explains the choice of a smaller than 1 exponent for $|x - c|$ in

$$\begin{aligned} L(x) &= \Pi(x) - \varepsilon(\ell_0 - \ell_1\varrho) - x \\ &= \big[1 - (\varepsilon(\ell_0 - \ell_1\varrho) + c)\big]\varepsilon^{b_1}|\varrho|^{b_2}\frac{1 - |x - c|^{1+a_1\varepsilon\varrho}}{\varepsilon^{b_1}|\varrho|^{b_2} + |x - c|}. \end{aligned}$$

The factor ϱ in the exponent accounts for the property that the further ϱ is below $V_{\rm spk}$, the orbit through c becomes flatter at p^*. The other property that $L(x)$ must decay rapidly as x moves away from the left side of c is accounted for by the factor $\varepsilon^{b_1}|\varrho|^{b_2}$. The property that $L(x) = 0$ at $\varrho = 0$ is consistent with the fact that $C_{\rm cpt}$ is a source for the CV-dynamics and the return of the upper branch of the strong unstable manifold defines the upper bound of Π instead of $R_{\max}$. The section wedged between the strong unstable manifold and the V-nullcline is instantaneously blocked out for orbits through $[R_{\min}, C_{\rm cpt}]$ at $\varrho = 0$.

As concluded above, Π is increasing in $[c, .5]$ and decreasing in $[.5, 1]$, that is $C_{\rm cpt} = .5$ is the only critical point in $[c, 1]$ and it is a local maximum. The reason that Π has a horizontal tangent line at $C_{\rm cpt} = .5$ follows the same argument as above for the relationship between points C_0 and C_1 near p^* except that C_0 is treated as dependent on C_1 in the case. The constraint $0 < \ell_2 < 1$ implies that $\Pi(1) = e^{-b_3/\varepsilon}(1 - \ell_3) > 0$, consistent with the fact that by following the defining CV- and nV-orbits for Π, point $R_{\max}$ returns to $\mathcal{J}_1$ above $R_{\min}$.

One shortcoming of the analytic model (2.2) is the absence of the property that at $\varrho = 0$, the derivative of Π should also have a limiting infinity at $.5^-$ because $C_{\rm cpt}$ is a source for the CV-equations and the left limit $.5^-$ corresponds to the upper strong unstable manifold of the source. In fact, $\Pi(x) = O(|x - .5|^{1-\varepsilon/\lambda})$ for x near $.5$, where constant $\lambda > 0$ is one eigenvalue of the linearization of the CV-vector field at the source $C_{\rm cpt}$ assuming ε is the other one. The same comment also applies to the right limit $.5^+$. We could make modifications to accommodate this property but the complications are not worthwhile and unnecessary for this paper.

References

1. Adrian, E.D., The Basis of Sensation: The Action of the Sense of Organs, W.W. Norton, New York, 1928.
2. Baesens, C., J. Guckenheimer, S. Kim, and R.S. MacKay, *Three coupled oscillators: mode-locking, global bifurcations and toroidal chaos,* Physica D **49**(1991) 387-475.
3. Bullock, T.H., S. Hagiwara, K. Kusano, and K. Hegishi, *Evidence for a category of electroreceptior in the lateral line of gymontid fishes*, Science, **134**(1961), pp.1426–1427.
4. Chay, T.R., Y.S. Fan, and Y.S. Lee, *Bursting, spiking, chaos, fractals, and universality in biological rhythms,* Int. J. Bif. & Chaos, **5**(1995), pp.595–635.
5. Collet, P. and J.-P. Eckmann, Iterated Maps of Interval as Dynamical Systems, Birkhauser, 1980.
6. de Melo, W. and S. van Strien, One-dimensional Dynamics, Springer-Verlag, Berlin, 1993.
7. Deng, B., *Homoclinic bifurcations with nonhyperbolic equilibria,* SIAM. J. Math. Anal., **21**(1990), pp.693–719.
8. Deng, B., *A mathematical model that mimics the bursting oscillations in pancreatic β-cells,* Math. Biosciences **119**(1993), pp.241–250.
9. Deng, B., *Glucose-induced period-doubling cascade in the electrical activity of pancreatic β-cells,* J. Math. Bio., **38**(1999), pp.21–78.
10. Feigenbaum, M., *Quantitative universality for a class of nonlinear transformations,* J. Stat. Phys., **19**(1979), pp.25–52.
11. Feigenbaum, M., *The universal metric properties of nonlinear transformation,* J. Stat. Phys., **21**(1979), pp.669–709.
12. Guckenheimer, J., R. Harris-Warrick, J. Peck, and A. Willms, *Bifurcation, bursting and spike frequency adaptation,* J. Comput. Neurosci. **4**(1997), pp.257-277.
13. Guckenheimer, J. and P. Holmes, Nonlinear Oscillations, Dynamical Systems, and Bifurcation of Vector Fields, Springer Verlag, 1983.
14. Hodgkin, A.L. and A.F. Huxley, *a quantitative description of membrane current and its application to conduction and excitation in nerve,* J. Physiol. **117**(1952), pp.500–544.
15. Hagiwara, S. and H. Morita, *Coding mechanisms of electroreceptor fibers in some electric fish,* J. Neurophysiol. **26**(1963), pp.551–567.
16. Perkel, D.H., T.H. Bullock, *Neural coding*, Neurosci. Res. Prog. Sum. **3**(1968), pp.405–527.
17. Poznanski, R.R., Modeling in The Neurosciences: from Ionic Channels to Neural Networks, Harwood Acadmic Pub., Amsterdam, The Netherlands, 1999.
18. Rieke, F., D. Warland, R. de Ruyter van Steveninck, W. Bialek, Spikes, Spikes: Exploring the Neural Code, The MIT Press, Cambridge, MA, 1996.
19. Rinzel, J., *A formal classification of bursting mechanisms in excitable systems,* Proc. Intern. Congr. of Mathematicians (A.M. Gleason, ed.), Amer. Math. Soc., pp.1578–1594.
20. Sherman, A., P., Carroll, R.M. Santos, and I. Atwater, *Glucose dose response of pancreatic β-cells: experimental and theoretical results,* in Transduction in Biological Systems, eds., C. Hidalgo, J. Bacigalupo, E. Jaimovich, and J. Vergara, pp.123–141, Plenum Publishing Co, 1990.
21. Terman, D., *Chaotic spikes arising from a model of bursting in excitable membranes,* SIAM J. Appl. Math., **51**(1991), pp.1418–1450.
22. Wang, X.-J. and J. Rinzel, *Oscillatory and bursting properties of neurons,* The Handbook of Brain Theory and Neural Networks, M. Arbib, ed., MIT Press, pp.686–691.

Department of Mathematics and Statistics, University of Nebraska-Lincoln, Lincoln, NE 68588, USA

Current address: Department of Mathematics and Statistics, University of Nebraska-Lincoln, Lincoln, NE 68588

E-mail address: `bdeng@math.unl.edu`